

Parma, 23 maggio 2017



SERVIZIO SANITARIO REGIONALE
EMILIA-ROMAGNA
Azienda Ospedaliero - Universitaria di Parma

Il ruolo di nuove tecniche di imaging per la diagnosi precoce di demenza

Livia Ruffini

*SC Medicina Nucleare
Azienda Ospedaliero-Universitaria di Parma*

PET AND SPECT STUDIES OF THE BRAIN

A. Different tracers to determine

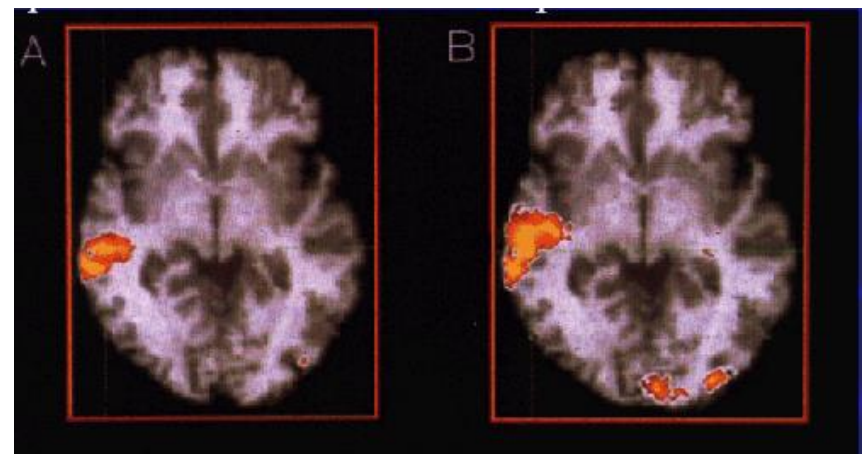
- Perfusion
- Glucose utilization
- Dopaminergic function
- Neuroreceptors ligands behaviour
- Aminoacide transport

B. Kinetic model of tracer

C. Quantitative maps of regional in vivo

- physiology
- biochemistry
- pharmacology

Molecular Imaging has substantially contributed to characterizing and better understanding the brain pathology underlying the motor and cognitive manifestations of ND



MOLECULAR IMAGING IN NEURODEGENERATIVE DISEASES

✓ Setting

- disease severity as reflected by presynaptic dopamine terminal dysfunction or amyloid load → decision making
- subclinical dysfunction in subjects who are at risk for ND
- management and follow-up
- disease progression and monitoring drug efficacy

✓ Imaging tools with increasing complex application (hybrid imaging)

SPECT → SPECT/CT → PET/CT → PET/MRI fusion

✓ Adding CT/MRI enhances accuracy and interobserver agreement

Advantages

- ✓ Quantifies specific molecular targets down to sub-nanomolar levels
- ✓ Links biological processes to symptoms and other clinical outcomes
- ✓ Enables treatments to be evaluated and monitored
- ✓ Enable translational approaches

SPECT

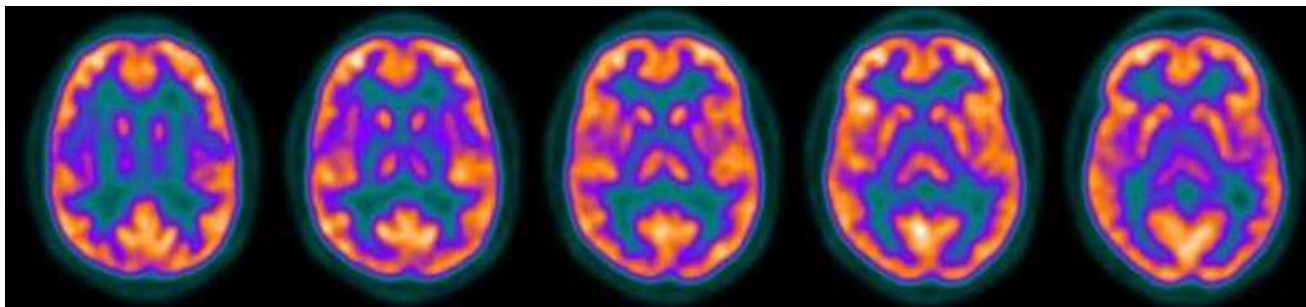


PET

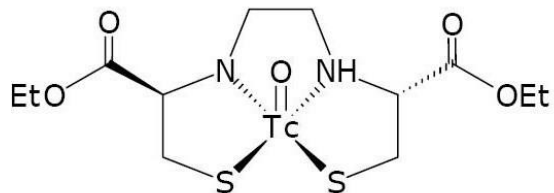
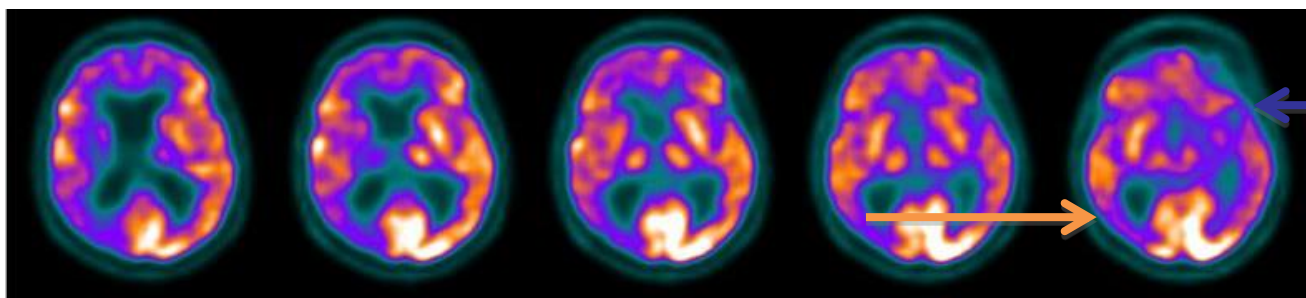


Brain perfusion: [99mTc]HMPAO, [99mTc]ECD SPECT

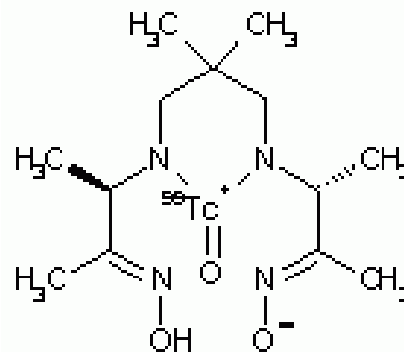
normal



Vascular disease



[99mTc]ECD

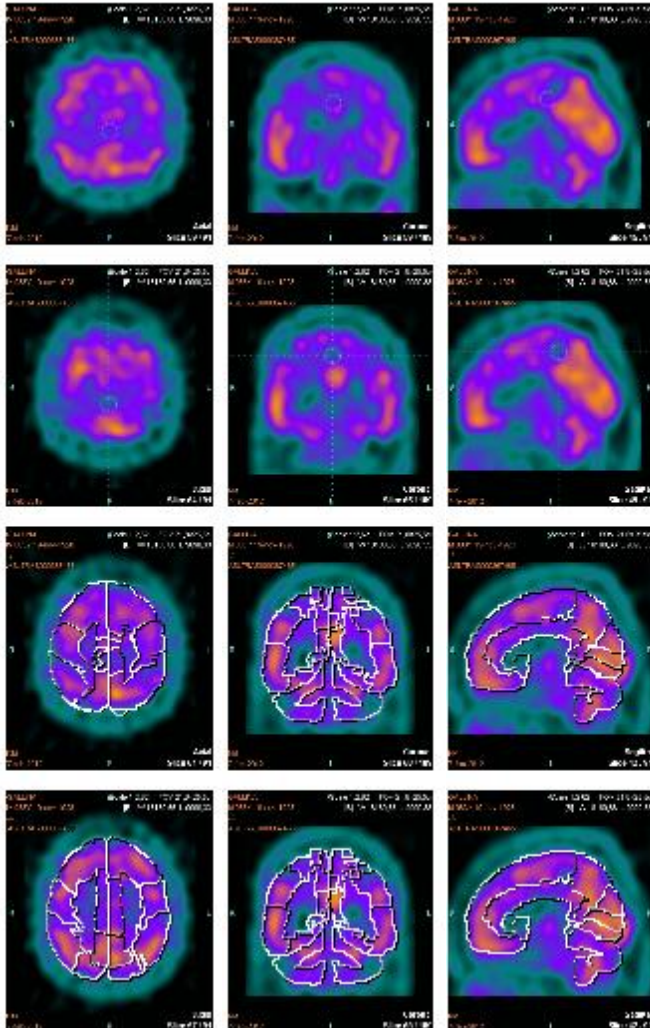


[99mTc]HMPAO

QUANTITATIVE ANALYSIS

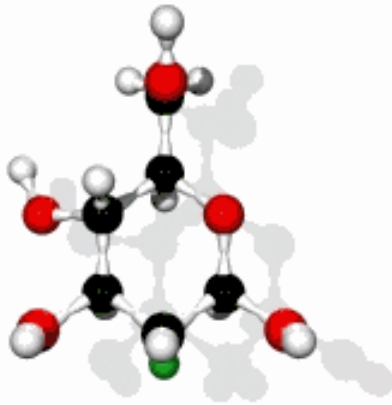
Method: Siemens Scenium analysis

✓ Voxel segmental analysis

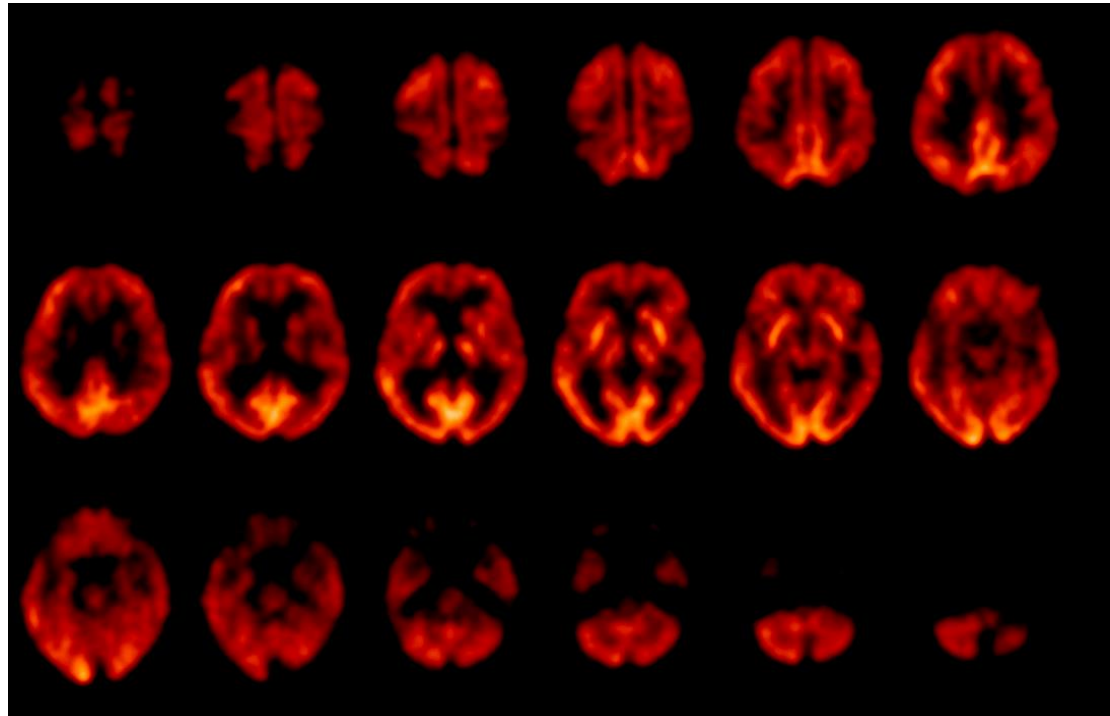


Region of Interest	Side	Min Uptake	Mean Uptake	Max Uptake	Mean # Std. Dev.
Basal ganglia	L	4.552	9.549	12.992	0,7
Basal ganglia	R	3.216	9.025	13.593	-0,3
Central region	L	4.607	9.649	13.074	2,1
Central region	R	4.436	9.614	13.701	3,2
Cerebellum	L	1.286	10.162	15.361	-0,3
Cerebellum	R	1.804	10.315	16.184	0,9
Cingulate and paracingulate gyri	L	5.516	10.247	14.464	3,8
Cingulate and paracingulate gyri	R	5.311	9.728	14.331	2,8
Frontal lobe	L	3.587	10.334	15.061	3,6
Frontal lobe	R	3.873	10.534	14.869	4,7
Mesial temporal lobe	L	6.060	8.627	11.193	1,1
Mesial temporal lobe	R	2.663	8.778	11.935	1,4
Occipital lobe	L	4.505	11.384	14.907	3,4
Occipital lobe	R	3.436	10.927	14.461	3,3
Parietal lobe	L	3.527	10.227	14.830	2,0
Parietal lobe	R	2.515	9.899	14.504	2,3
Temporal lobe	L	4.506	10.575	13.673	3,0

Cellular glucose utilization: $[^{18}\text{F}]\text{FDG}$ PET

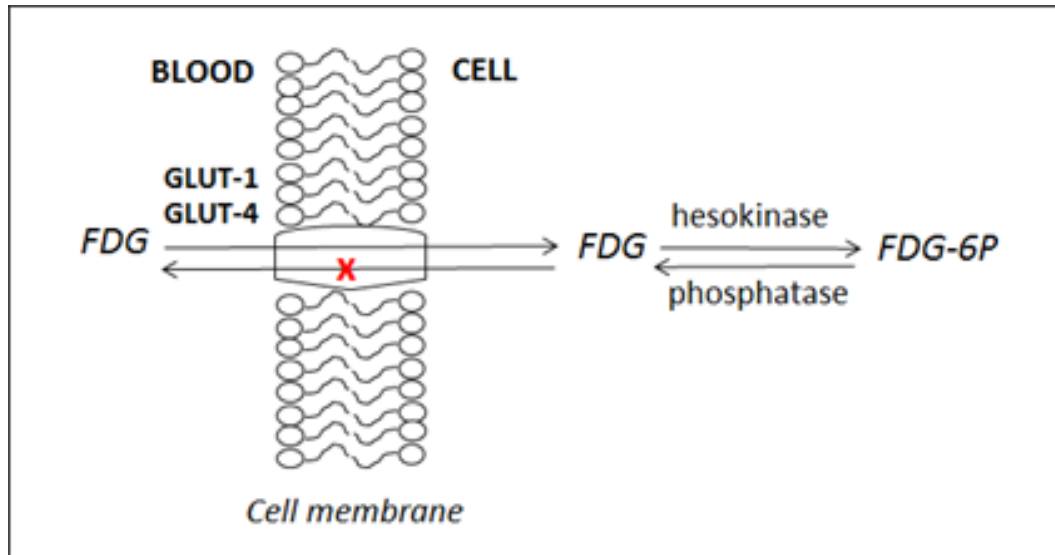


Radioactive Sugar

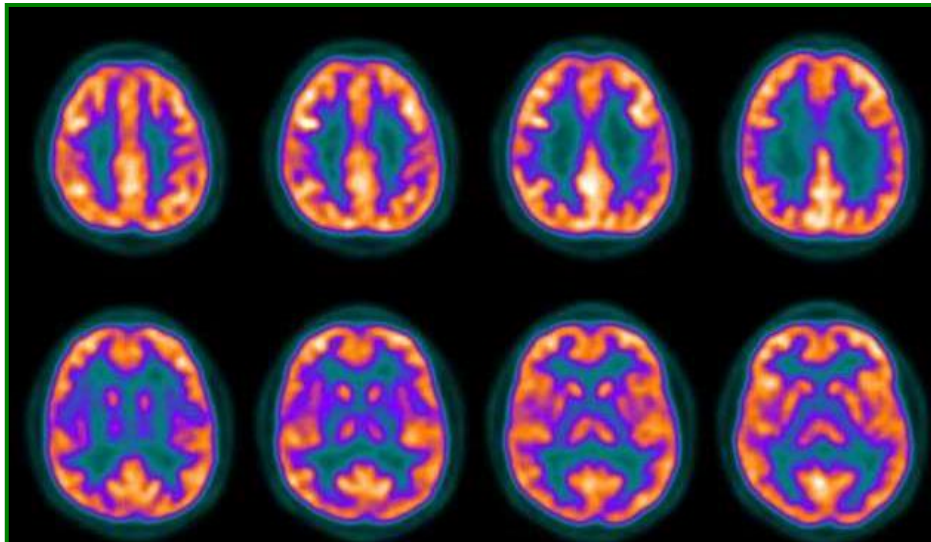


Normal brain and glucose consumption

Neuronal glucose utilization: FDG PET



- FDG PET images are most often normal in the early stage and by visual assessment



QUANTITATIVE ANALYSIS

The most widely used FDG PET analysis methods for neurology research include, among others:

Neurostat (University of Washington, Seattle)

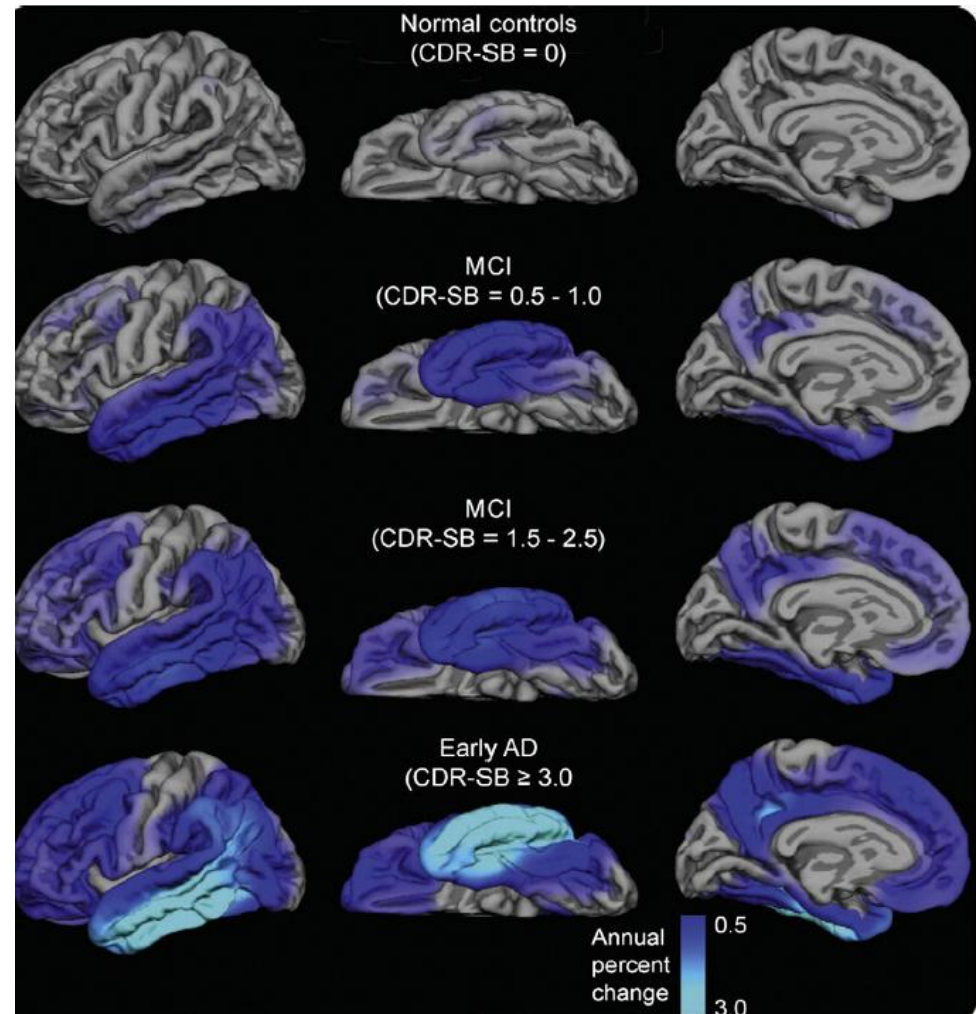
T-SUM tool implemented in PMOD
hypometabolic convergence indexes

Statistical Parametric Mapping
procedures (SPM; Wellcome

Department of Cognitive Neurology,
London, U.K.)

→ Spatial normalization procedures to enable voxel-based comparison of a patient's scans to a normative reference database

→ Yield statistical maps depicting deviations from norms at the individual voxel level, on a subject-by-subject basis

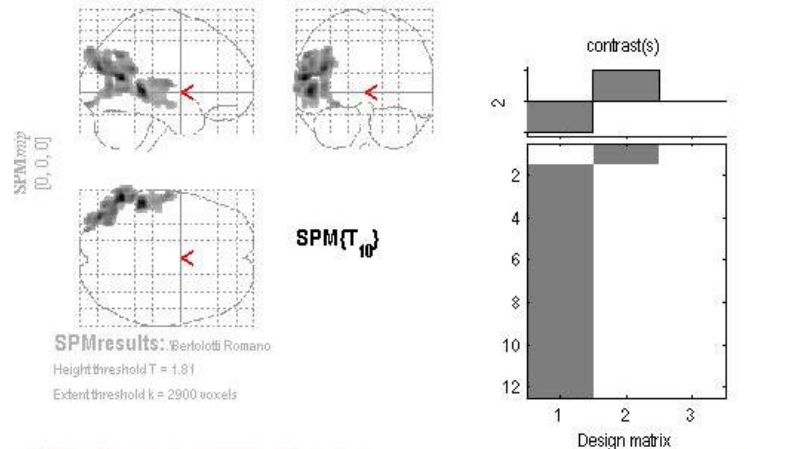


Annual atrophy rates as a function of degree of clinical impairment.

Atrophy rates are most prominent in posterior brain regions early in the course of disease, spreading to anterior regions as the level of impairment increases, with relative sparing of sensorimotor regions

QUANTITATIVE ANALYSIS

Method: PET-SPM5, SPM8 dedicated Software



Statistics: *p*-values adjusted for search volume

cluster-level			voxel-level					x,y,z (mm)		
$p_{\text{uncorrected}}$	k_E	$p_{\text{uncorrected}}$	p_{FWE}	p_{FDR}	T	(Z_{crit})	$p_{\text{uncorrected}}$			
0.070	2985	0.000	1.000	0.861	4.85	3.40	0.000	-60	-58	14
			1.000	0.861	4.51	3.26	0.001	-54	-38	0
			1.000	0.861	3.93	2.99	0.001	-40	-82	24

✓ Comparison of uptake value with normal control database

✓ P value < 0.01

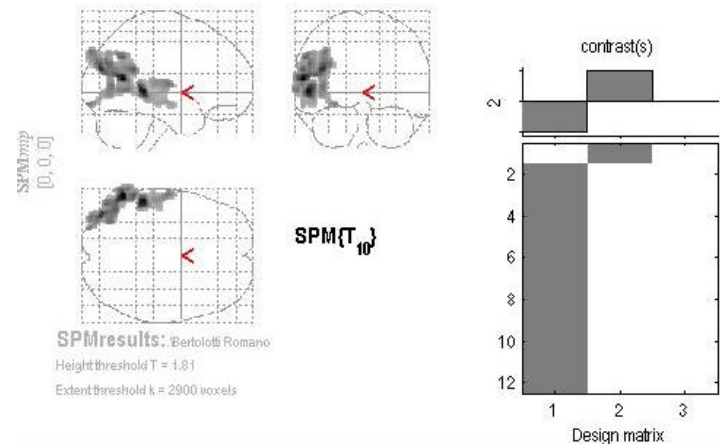
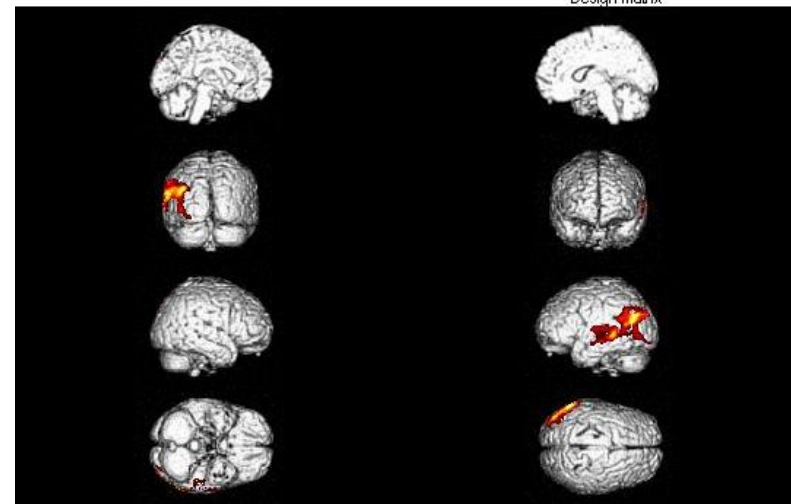
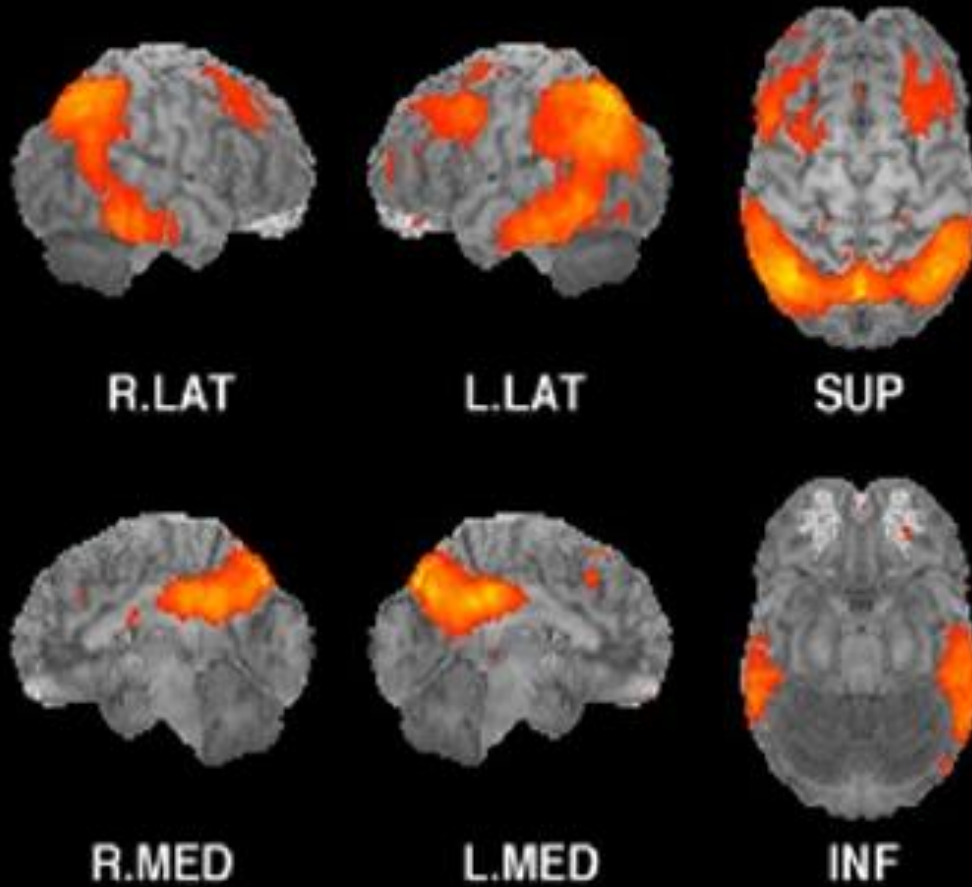


table shows 3 local maxima more than 8.0mm apart

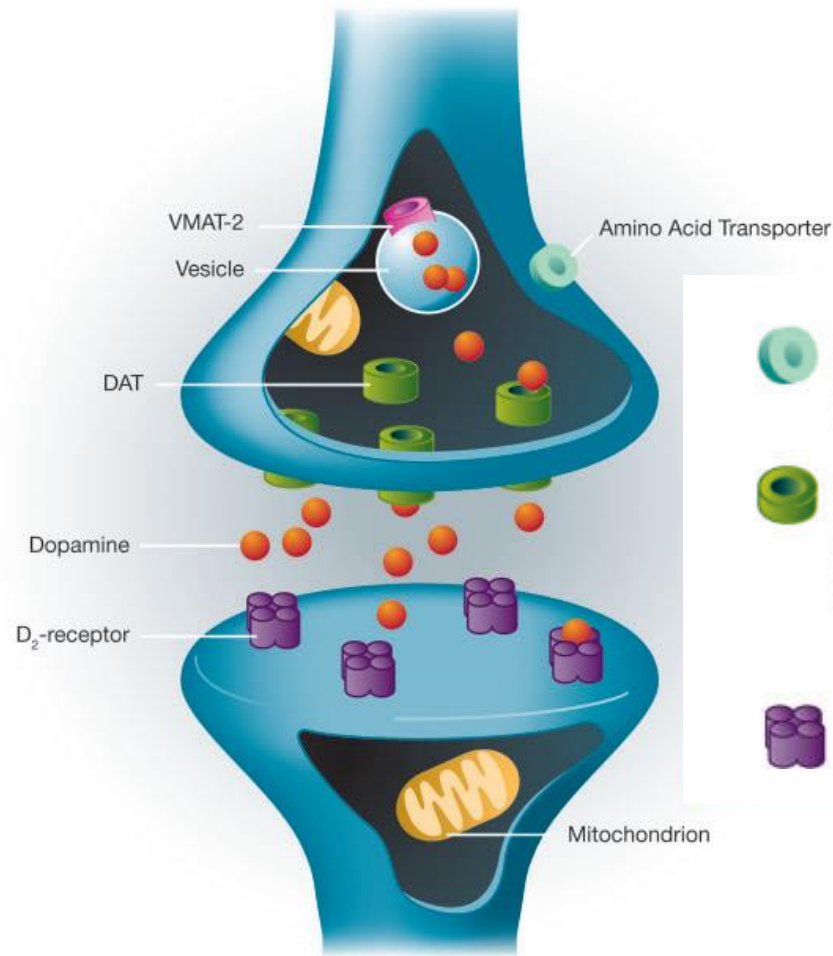
Height threshold: $T = 1.81$, $p = 0.049$ (1.000)	Degrees of freedom = [1.0, 10.0]
Extent threshold: $k = 2900$ voxels, $p = 0.000$ (0.081)	Smoothness FWHM = 11.4 12.2 13.2 (mm) = 5.7 6.1 6.6 (voxels)
Expected voxels per cluster, $<k> = 181.228$	Search vol: 4058312 mm ³ ; 507289 voxels; 2113.0 resels
Expected number of clusters, $<c> = 0.08$	Voxel size: [2.0, 2.0, 2.0] mm (1 resel = 230.98 voxels)
Expected false discovery rate, $<= 0.86$	






Quantitative evaluation of glucose rate uptake

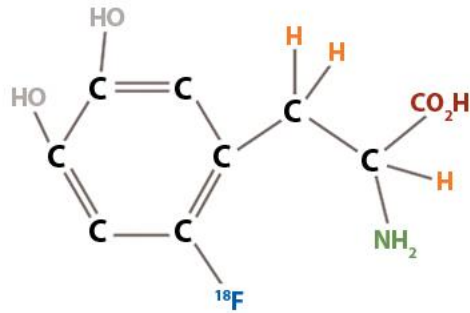


DOPAMINERGIC IMAGING



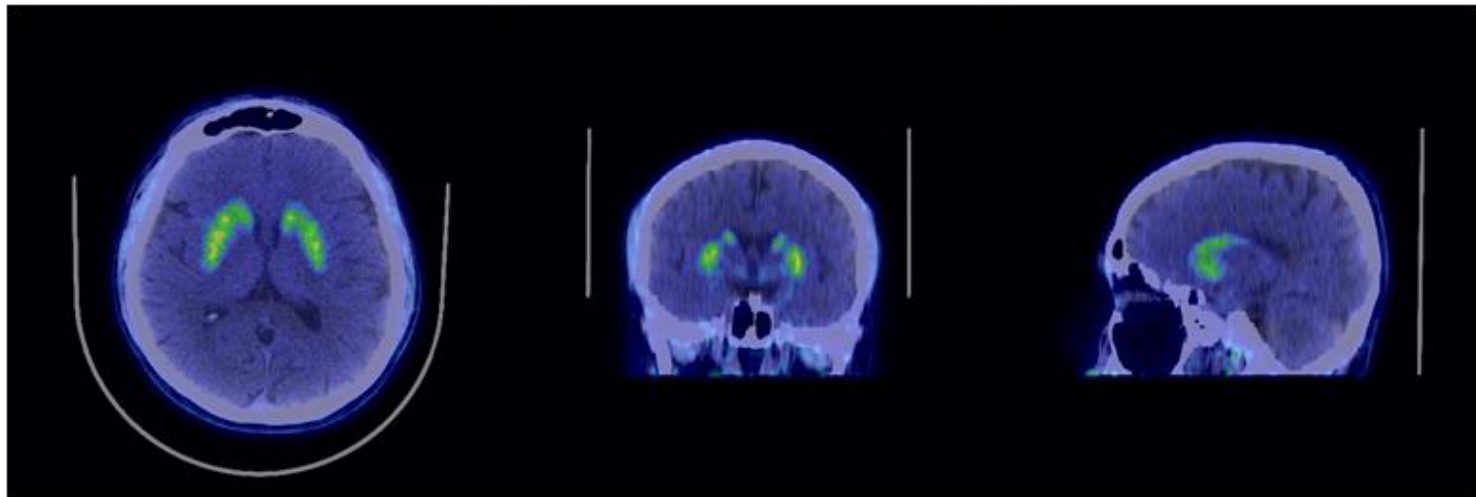
	Presynaptic radioligand	SPECT	PET
	DOPA decarboxylase activity (measures dopamine synthesis)		$[^{18}\text{F}]$ dopa
	DAT Ligand for dopamine transporter (provides measures of functioning dopaminergic terminals)	$[^{123}\text{I}]$ FP-CIT	
	Postsynaptic radioligands D2 receptor	$[^{123}\text{I}]$ IBZM	

DOPA decarboxylase activity: [^{18}F]DOPA PET



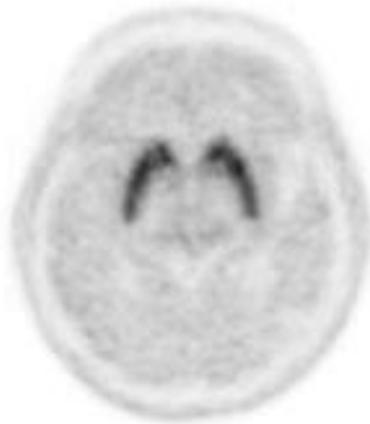
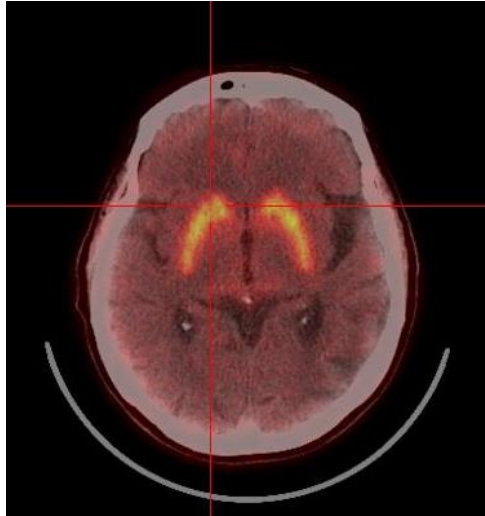
Functional state of dopamine
innervations in living brain
Pre-synaptic radioligand

PET/CT

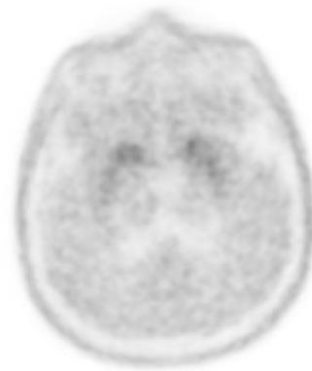
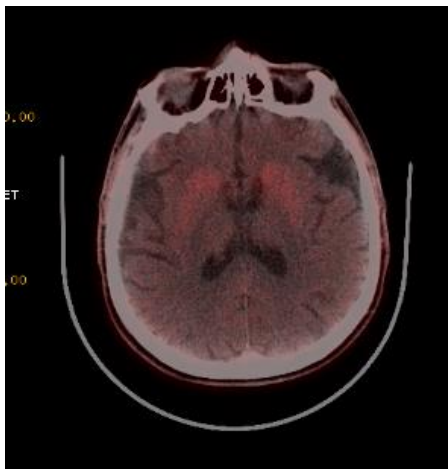


- Striatal [^{18}F]DOPA uptake has been shown to correlate with dopaminergic cell densities in the substantia nigra and with striatal dopamine levels.
- Uninfluenced by dopaminergic medication, suggesting the usefulness of [^{18}F]DOPA PET as a biomarker for monitoring the progression.

DOPA decarboxylase activity: [^{18}F]DOPA PET/CT



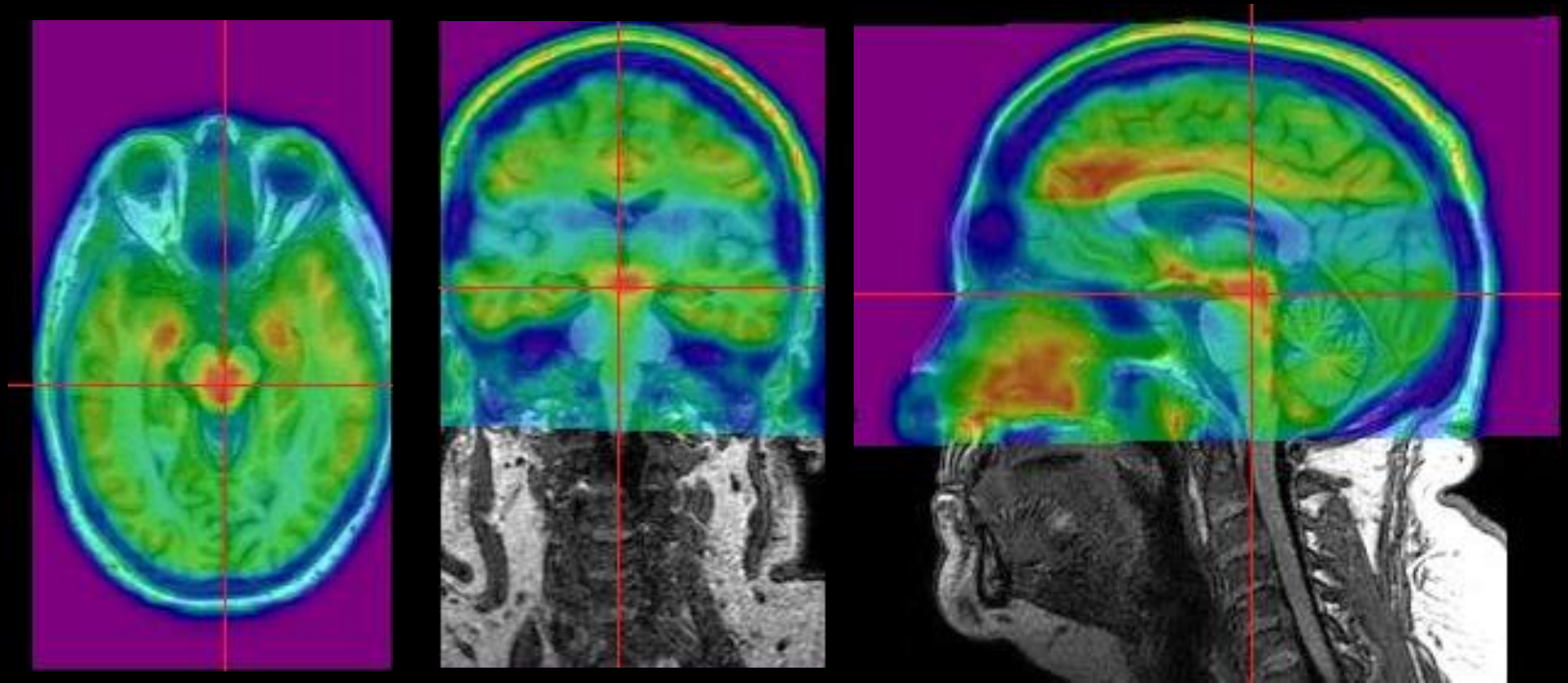
Drug induced tremor
Normal uptake



Advanced Parkinson's disease

Lower [^{18}F]DOPA uptake in the putamen has also been correlated with greater severity of motor symptoms and greater severity of bradykinesia and rigidity in PD

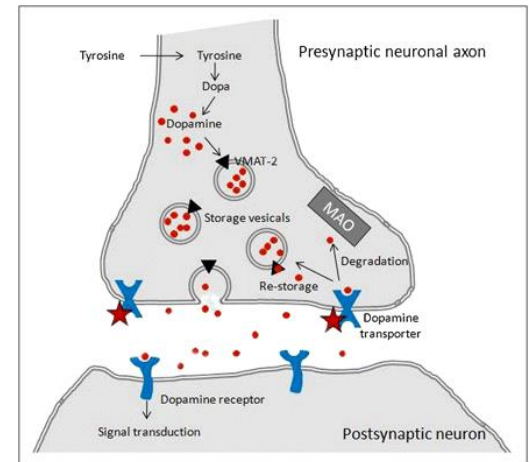
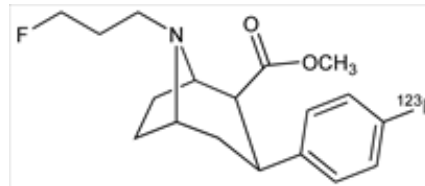
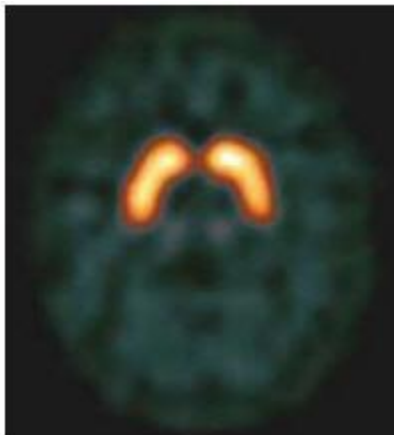
[¹⁸F]dopa PET/MR fusion
Dynamic PET imaging



PD
Restless leg syndrome

Dopamine transporter (DAT): [¹²³I]FP-CIT SPECT (DatScan)

- ✓ DAT is a sodium chloride-dependent transmembrane protein
- ✓ DAT controls dopamine levels by active reuptake of dopamine from the synaptic cleft after its interaction with the postsynaptic receptor
- ✓ Striatal 123I-FP-CIT uptake is correlated with DAT density



Europe

2000 authorized for clinical use for the differential diagnosis of patients with clinically uncertain Parkinsonian syndrome

2006 expanded for the differential diagnosis of probable dementia with Lewy bodies from Alzheimer disease

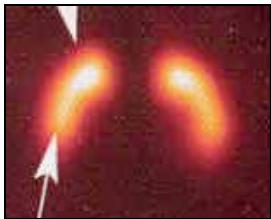
USA

2011 FDA approval of ¹²³I-FP-CIT for clinical use

Visualization of the presynaptic DAT distribution in the striatum

Dopamine transporter (DAT): [^{123}I]FP-CIT SPECT

Functional integrity of dopaminergic nerve
terminals in the striatum
Pre-synaptic radioligand



Normal



H&Y 1



H&Y 2



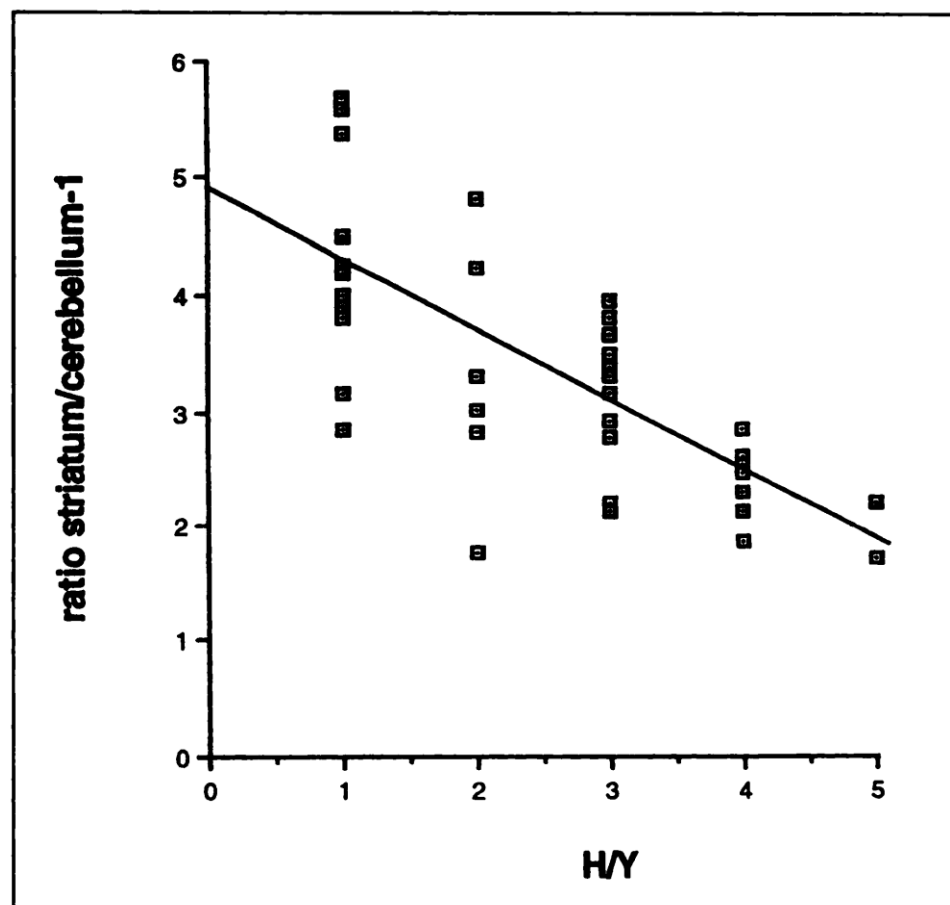
H&Y 3

Biomarker of Parkinson disease progression (related to the Hoehn & Yahr rating scale)

Annual rate of reduction of striatal DAT uptake 6 - 13% in PD patients
(versus 0 to 2.5% in healthy controls)

Correlation between [123I]FP-CIT binding ratio and clinical severity of locomotor disability

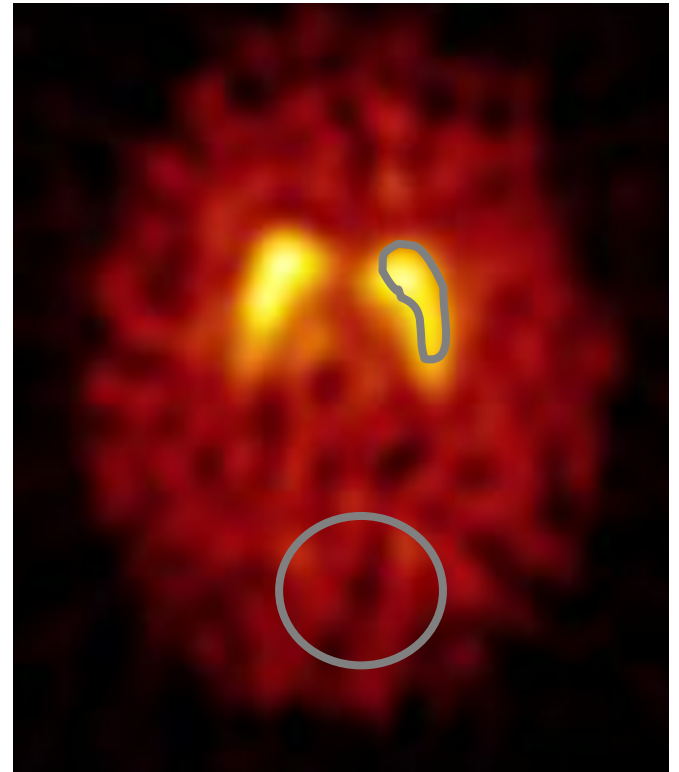
Putamen uptake of [123I]FP-CIT inversely correlates with Unified Parkinson's Disease Rating scale (UPDRS)



ROI (Region of Interest) method for quantification

Striatum/posterior cortex binding ratio

Striatum ROI cnts/ occipital ROI cnts %

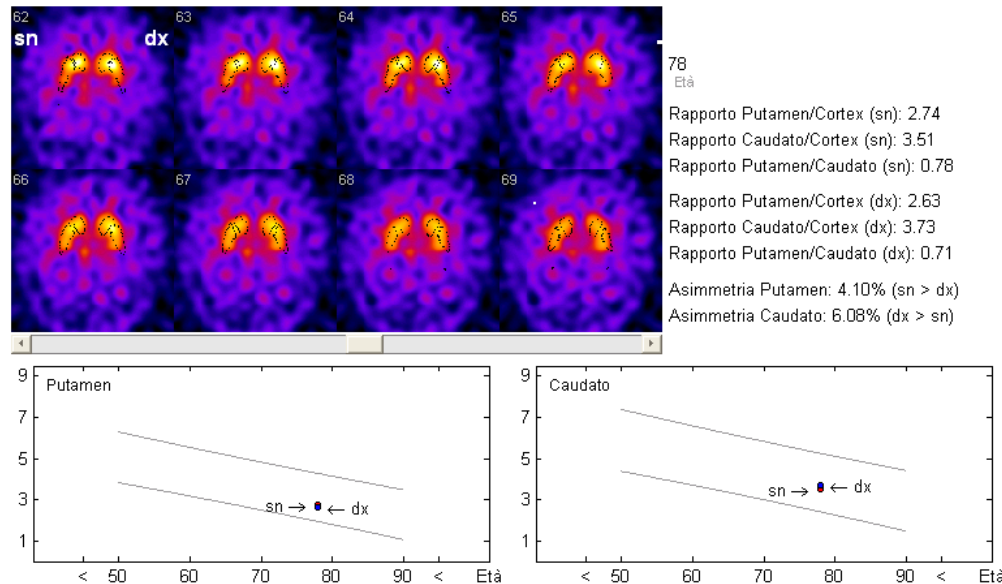


QUANTITATIVE ANALYSIS

Method: Basal Ganglia dedicated Software

Eur J Nucl Med Mol Imaging (2007)

U.O. MEDICINA NUCLEARE - AZIENDA OSPEDALIERO-UNIVERSITARIA DI PARMA ANALISI SEMIQUANTITATIVA CON METODO BASAL GANGLIA

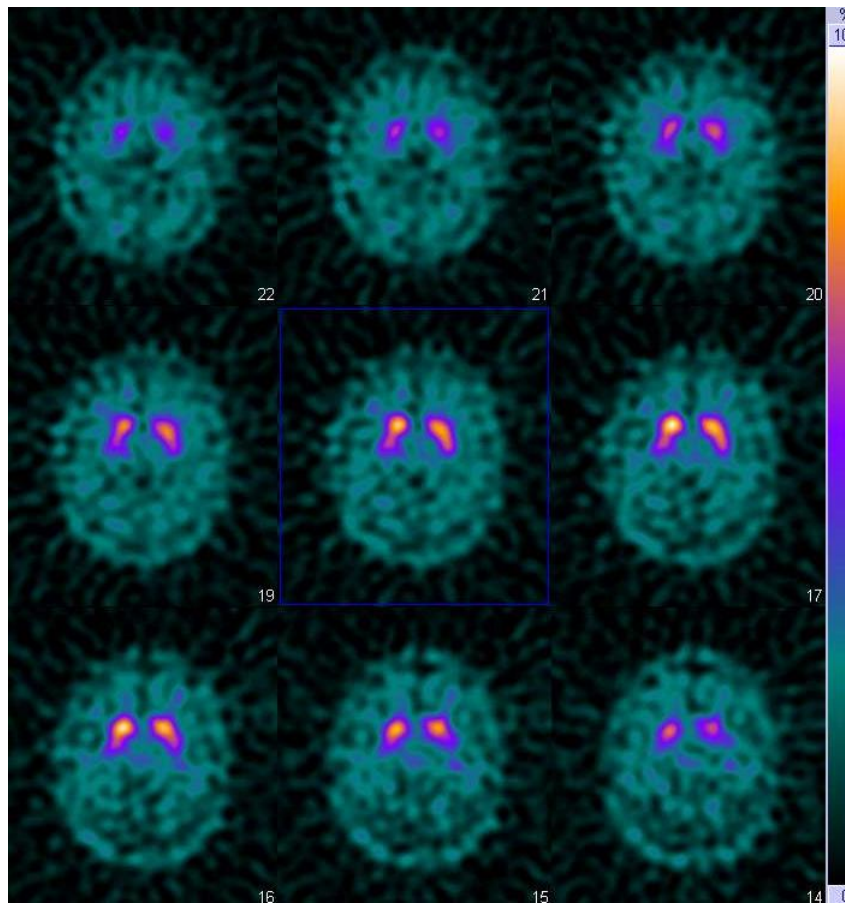


I risultati dell'esame del paziente sono rappresentati su di un grafico costruito analizzando con il metodo *Basal Ganglia* una popolazione non parkinsoniana di 50 soggetti (studio multicentrico). Le linee grigie rappresentano, all'interno della fascia di età tra 50 e 90 anni, i limiti di normalità con una confidenza del 90%.

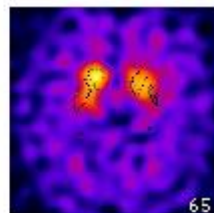
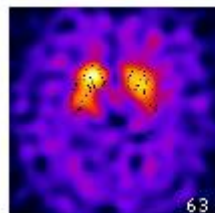
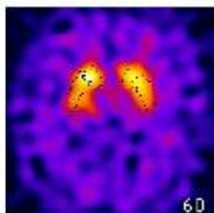
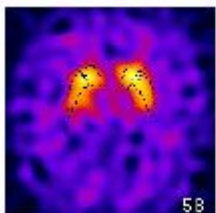
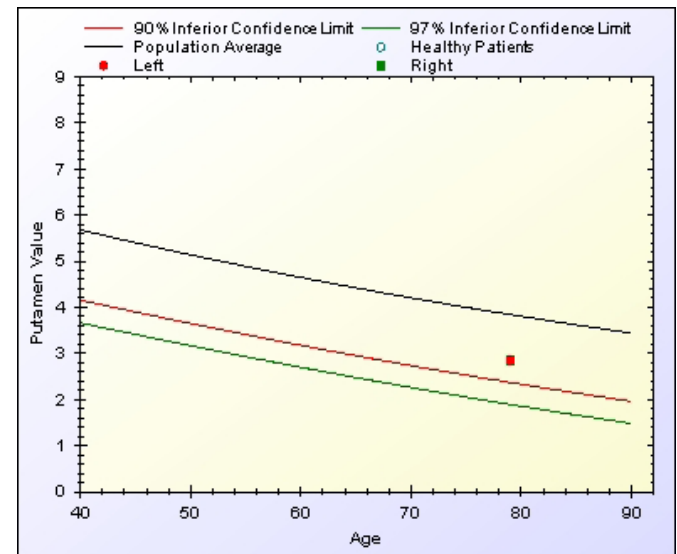
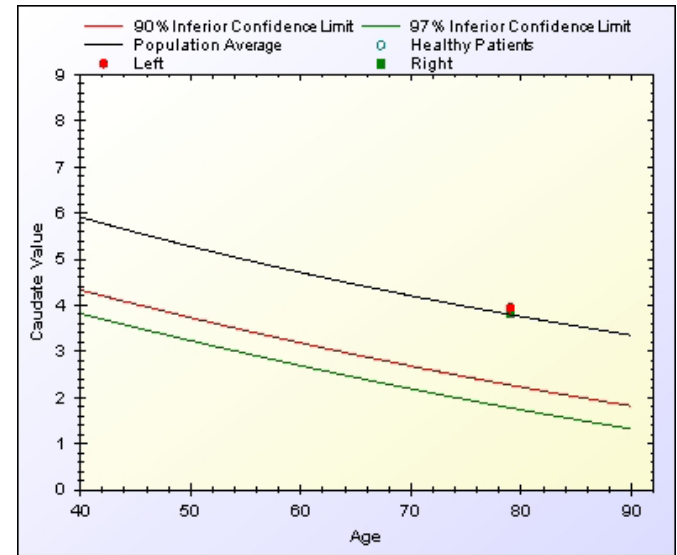
- ✓ 3D method for striatal automatic segmentation with anatomical reference in the Talairach e Tournoux atlas
- ✓ Comparison of uptake value with normal control database.

QUANTITATIVE ANALYSIS

Method: Basal Ganglia dedicated Software

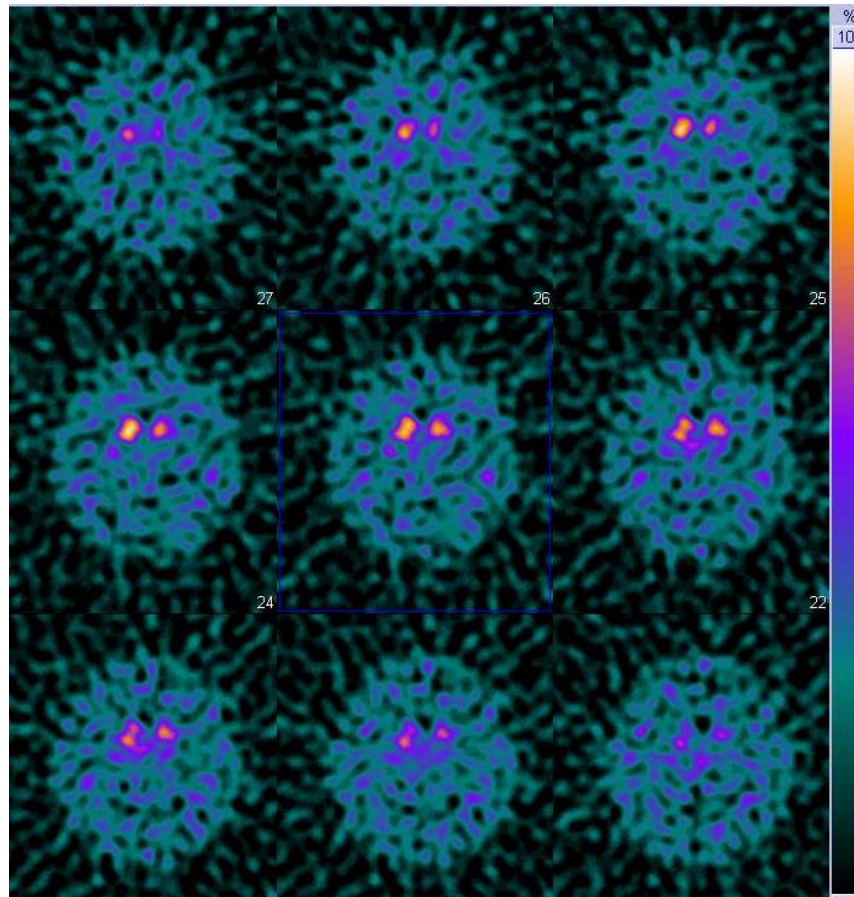


M, 64 yr
Right hand
tremor

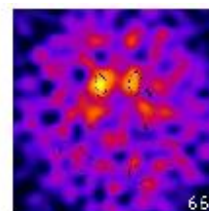
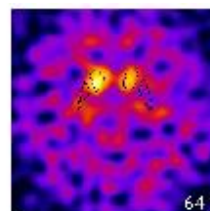
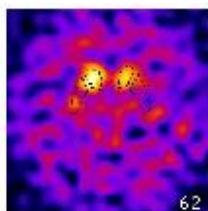
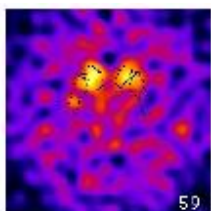
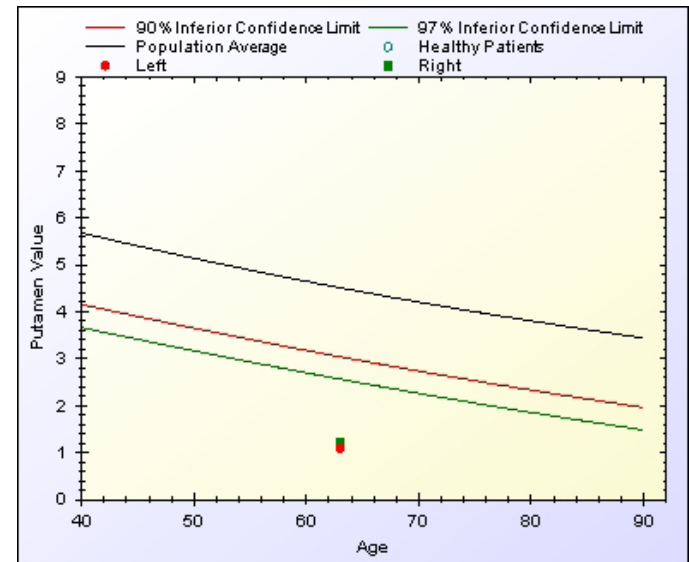
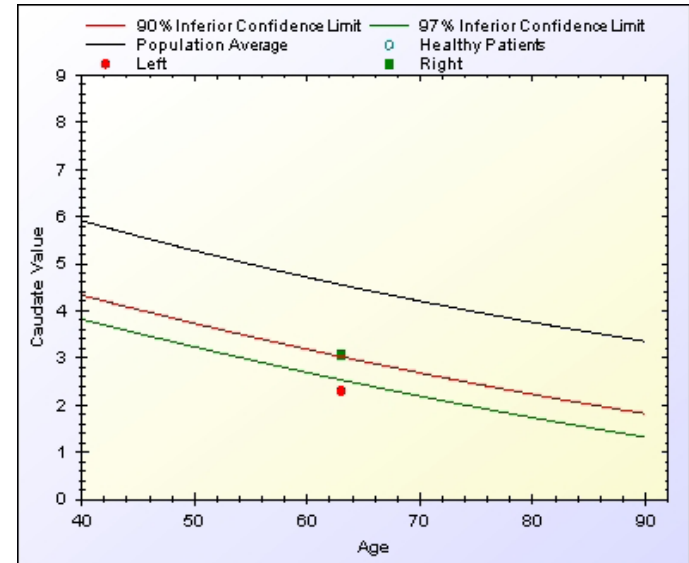


QUANTITATIVE ANALYSIS

Method: Basal Ganglia dedicated Software

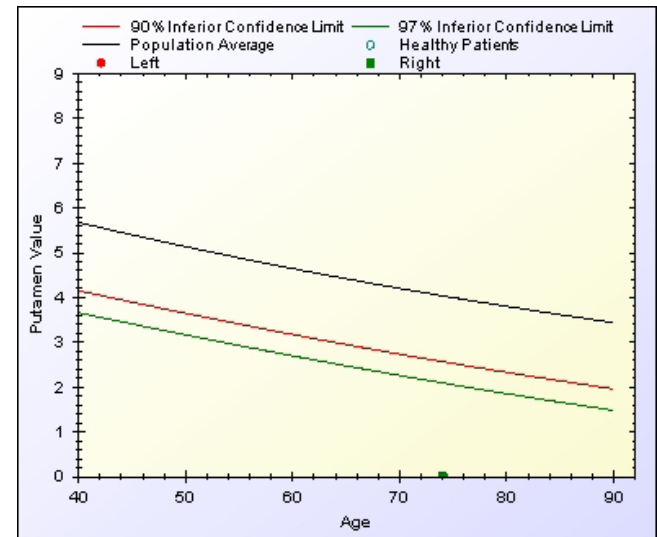
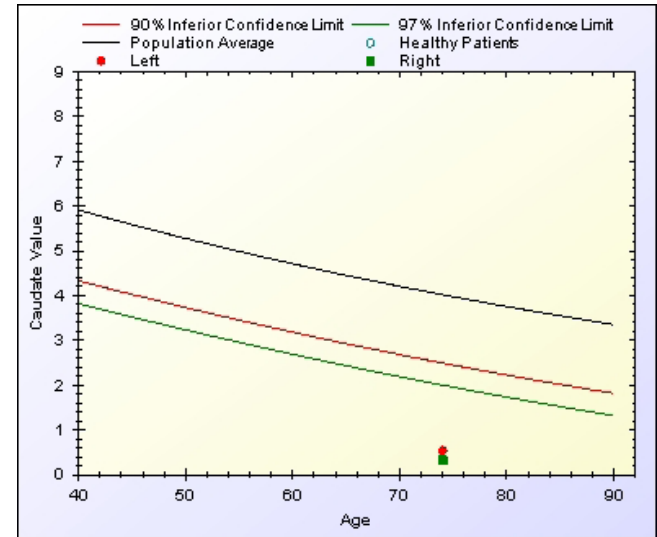
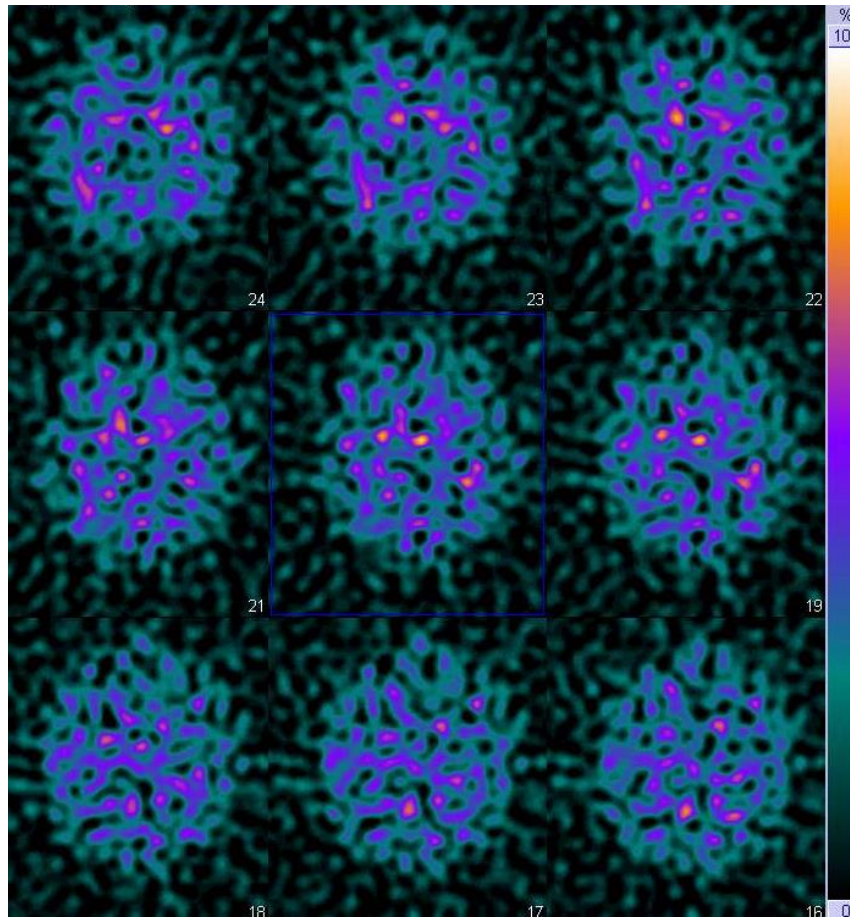


M, 60 yr
Hands
tremor and
bradikinesia



QUANTITATIVE ANALYSIS

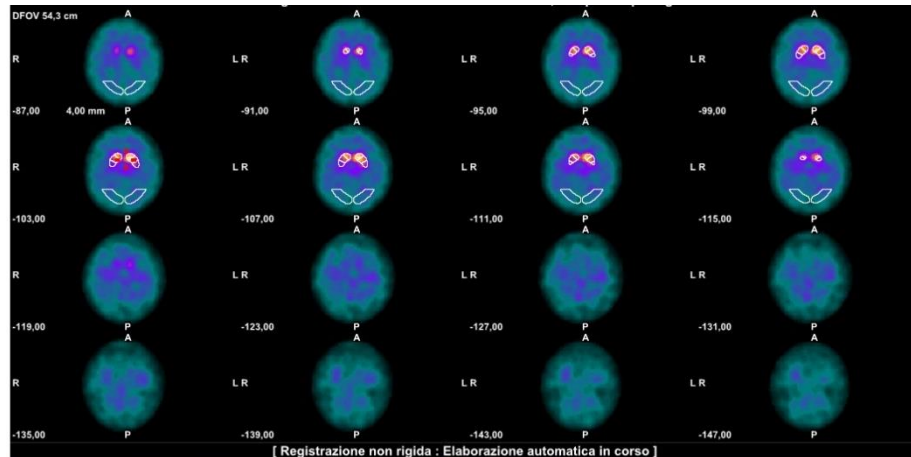
Method: Basal Ganglia dedicated Software



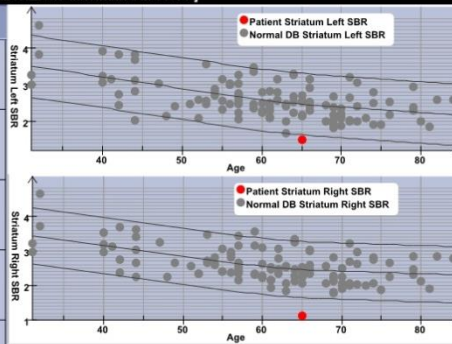
QUANTITATIVE ANALYSIS

Method: DatQuant® (GE Healthcare)

Certified for clinical trials
Normal population: 18-85 yrs

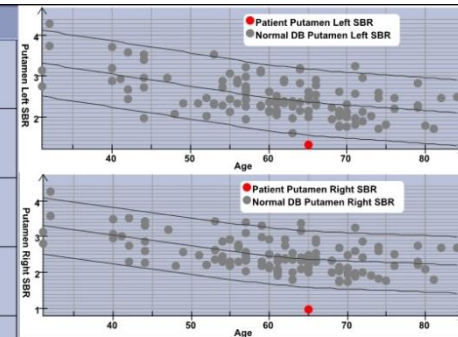


	Misurato	Media (± 1 SD)	Deviazione	Punteggio Z
Striatum Right SBR	+1,12	+2,46 ($\pm 0,40$)	-54%	-3,30
Striatum Left SBR	+1,49	+2,47 ($\pm 0,42$)	-40%	-2,33
Putamen Right SBR	+0,98	+2,38 ($\pm 0,39$)	-59%	-3,58
Putamen Left SBR	+1,31	+2,36 ($\pm 0,41$)	-45%	-2,58
Caudatus Right SBR	+1,46	+2,66 ($\pm 0,48$)	-45%	-2,48
Caudatus Left SBR	+1,85	+2,70 ($\pm 0,50$)	-31%	-1,69

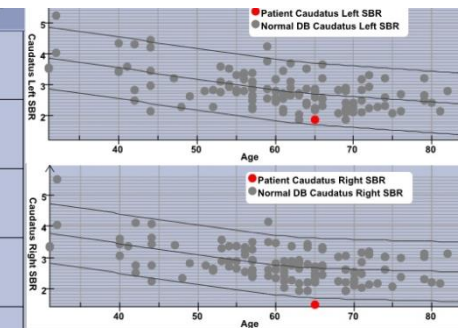


M, 68 yr
Right arm tremor and
rest leg syndrome

	Misurato	Media (± 1 SD)	Deviazione	Punteggio Z
Striatum Right SBR	+1,12	+2,46 ($\pm 0,40$)	-54%	-3,30
Striatum Left SBR	+1,49	+2,47 ($\pm 0,42$)	-40%	-2,33
Putamen Right SBR	+0,98	+2,38 ($\pm 0,39$)	-59%	-3,58
Putamen Left SBR	+1,31	+2,36 ($\pm 0,41$)	-45%	-2,58
Caudatus Right SBR	+1,46	+2,66 ($\pm 0,48$)	-45%	-2,48
Caudatus Left SBR	+1,85	+2,70 ($\pm 0,50$)	-31%	-1,69



	Misurato	Media (± 1 SD)	Deviazione	Punteggio Z
Striatum Right SBR	+1,12	+2,46 ($\pm 0,40$)	-54%	-3,30
Striatum Left SBR	+1,49	+2,47 ($\pm 0,42$)	-40%	-2,33
Putamen Right SBR	+0,98	+2,38 ($\pm 0,39$)	-59%	-3,58
Putamen Left SBR	+1,31	+2,36 ($\pm 0,41$)	-45%	-2,58
Caudatus Right SBR	+1,46	+2,66 ($\pm 0,48$)	-45%	-2,48
Caudatus Left SBR	+1,85	+2,70 ($\pm 0,50$)	-31%	-1,69



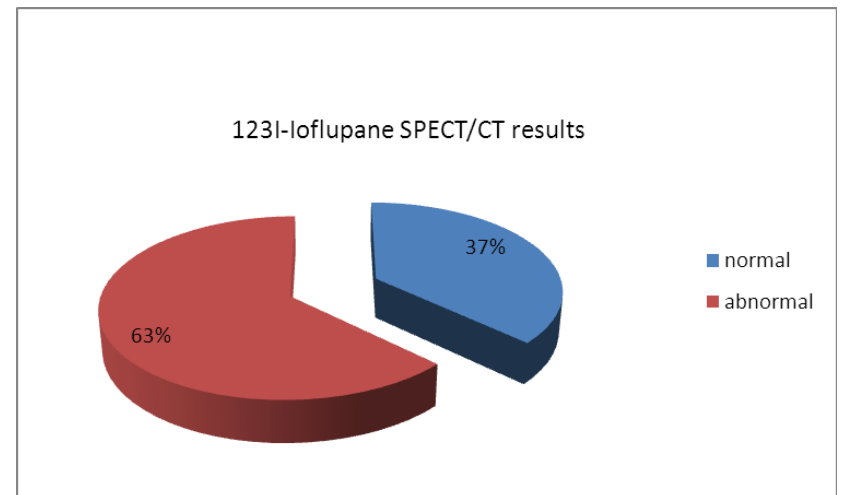
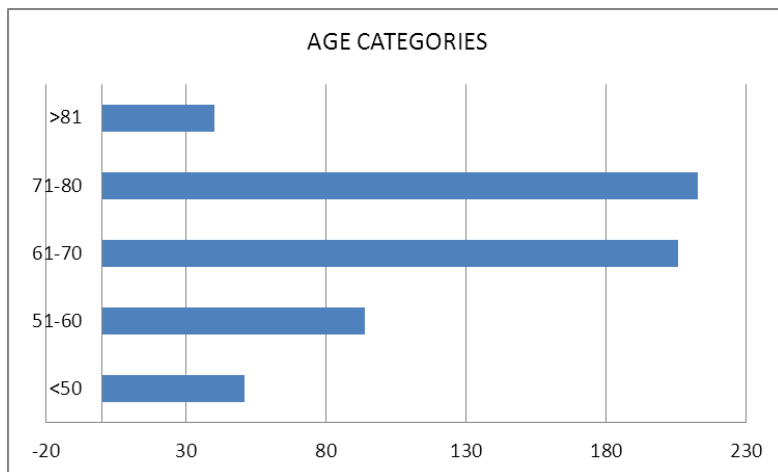
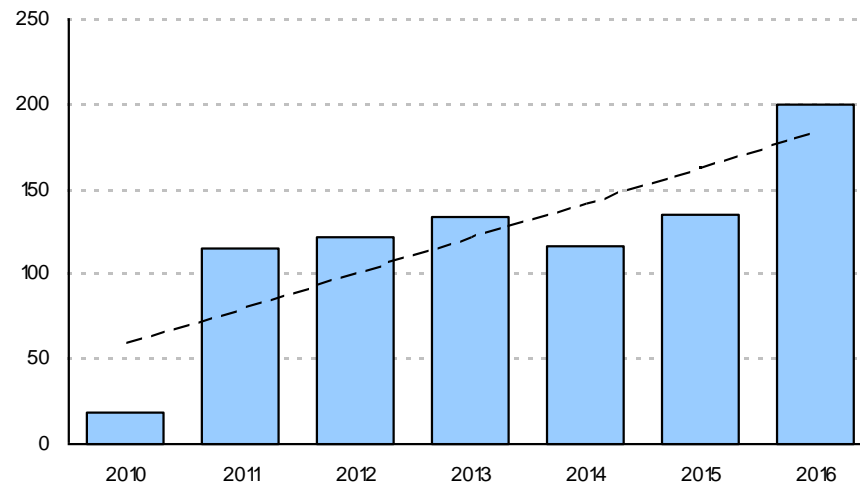
Drugs to be stopped for 4 wk before [¹²³I]FP-CIT SPECT

DRUG CLASS	DRUG NAME	EFFECT ON [¹²³ I]FP-CIT binding
COCAINE		↓
AMPHETAMINES	d-Amphetamine methamphetamine methylphenidate	↓
CNS STIMULANTS	Phentermine or ephedrine	↓ influences are likely when used as tablets
MODAFINIL		↓
ANTIDEPRESSANTS	Mazindol bupropion radafaxine	↓
ADRENERGIC AGONISTS	Phenylephrine or norepinephrine	↑ influences are likely when infused at high doses
ANTICHOLINERGIC DRUGS		Benztropine ↓ Other anticholinergics ↑ (which will likely not affect visual assess)
OPIOIDS	Fentanyl	↓
ANESTHETICS	Ketamine PCP Isoflurane	↓

Antiparkinsonian drugs including L-dopa, dopamine agonists, monoamine oxidase-B inhibitors, and catechol-O-methyl transferase inhibitors do not need to be discontinued.

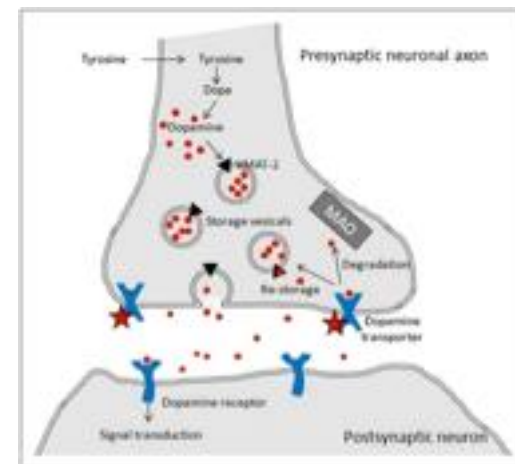
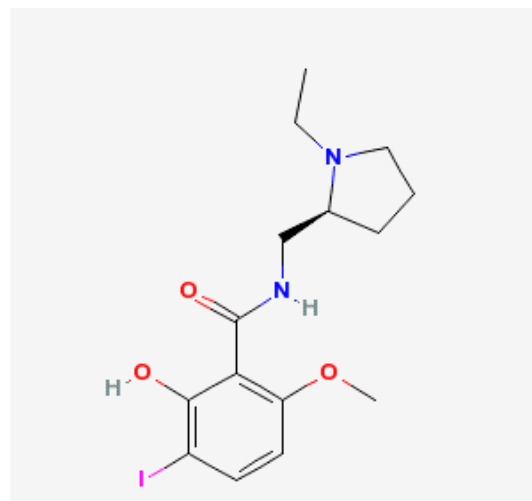
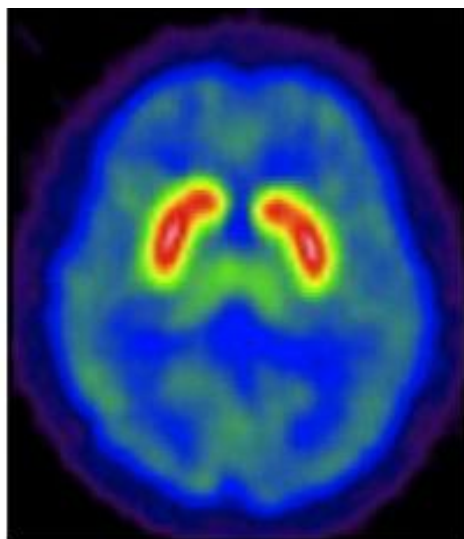
They showed no significant effect on the striatal ¹²³I-FP-CIT uptake.

DAT imaging at AOU-PR



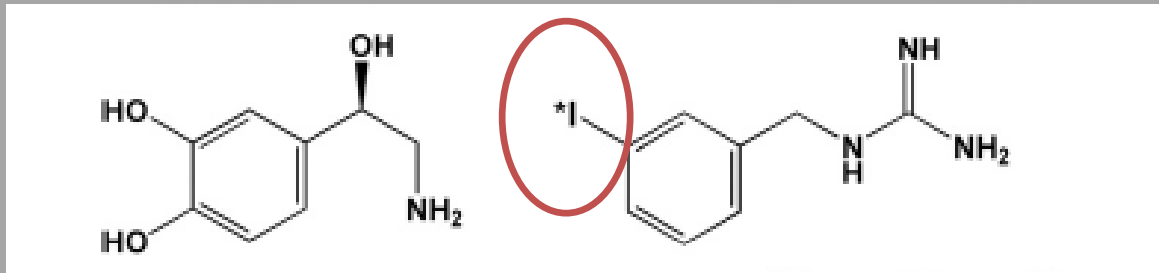
Dopamine receptor imaging D2/3R receptor: [^{123}I]IBZM SPECT

Postsynaptic radioligand
Selective D2/3R antagonist



- Upregulation of D2/3R in early PD
- Biomarker of the striatal dopaminergic reward system in obesity

Cardiac adrenergic innervation: ¹²³I-MIBG SPECT



NE

Metaiodobenzylguanidine

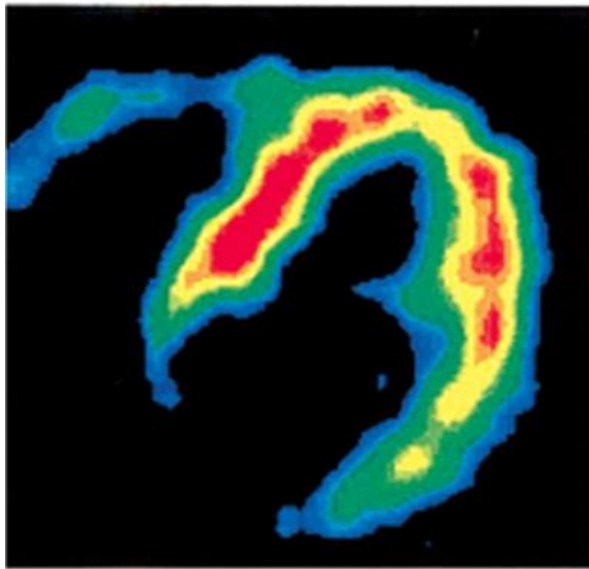
*I = I-131 o I-123 o I-124

- **1994** [¹³¹I]MIBG received Food and Drug Administration (FDA) approval (NDA 20-084) as an imaging agent
- **2008** [¹²³I]MIBG approved by FDA (NDA 22-290) as a tumor imaging agent (Adreview; GE Healthcare, Little Chalfont, UK).
- In Europe and Japan [¹²³I]MIBG and [¹³¹I]MIBG were approved for tumor imaging more than 10 years ago

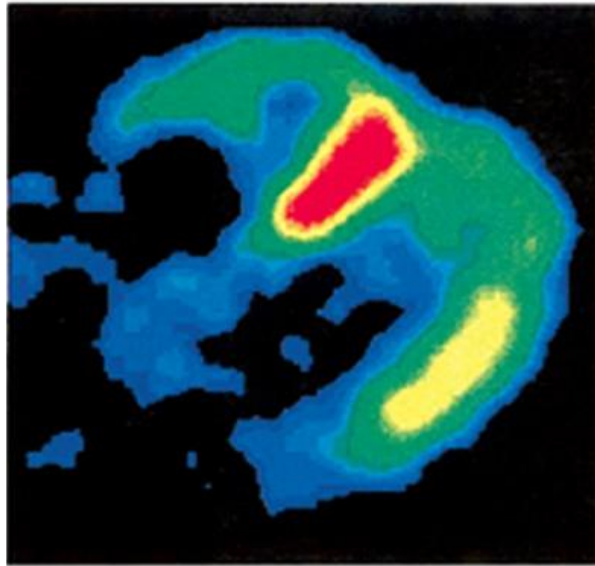
Progressive loss of uptake in Parkinson's disease

^{123}I -mIBG SPECT

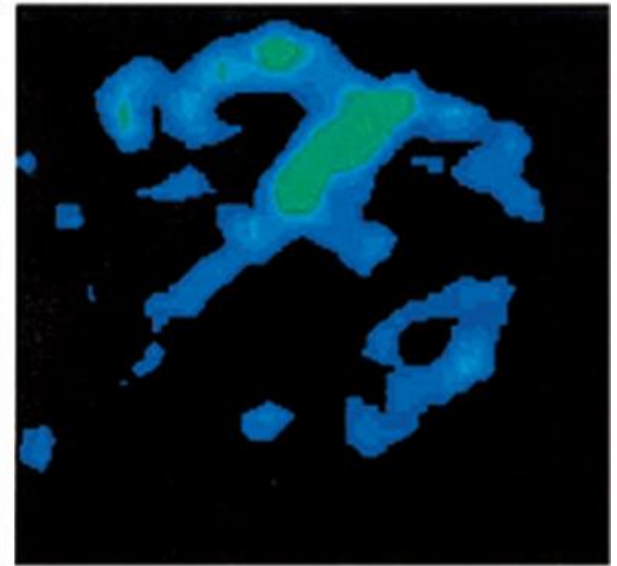
Normal



Parkinson



Baseline

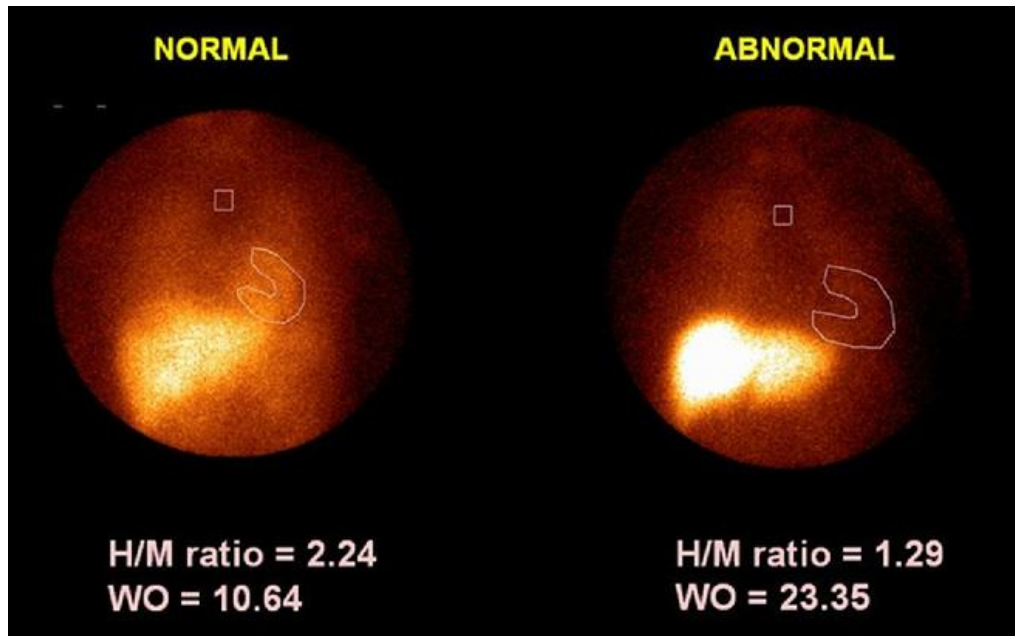


After 2 years

mIBG scanning

Early imaging
(15 min after injection)

Late imaging (4 hrs)

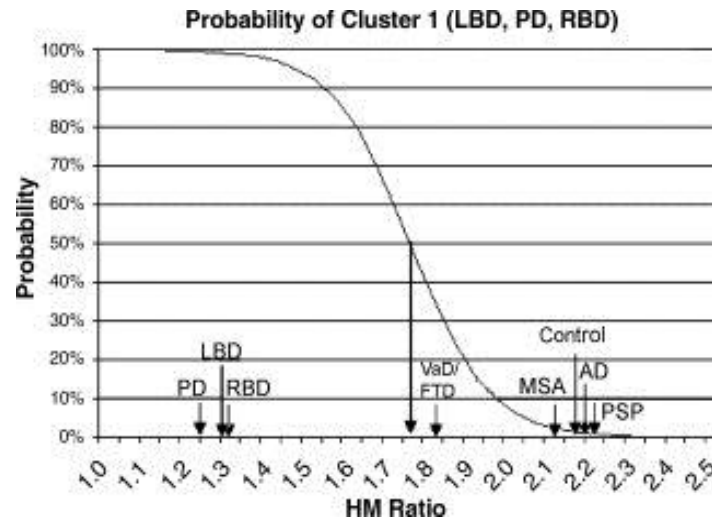


Early H/M reflects the integrity of presynaptic nerve terminals and uptake-1 function.

Late H/M combines information on neuronal function from uptake to release through the storage vesicle at the nerve terminals.

Washout is an index of the degree of sympathetic drive. Increased adrenergic drive is associated with high myocardial ^{123}I -MIBG washout and low myocardial ^{123}I -MIBG delayed uptake.

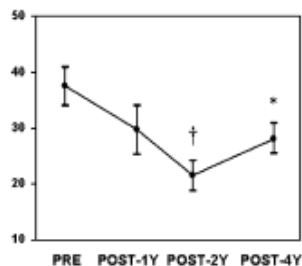
Meta-analysis of 123I-mIBG cardiac scintigraphy for the diagnosis of Lewy body–related (DLB and PD) disorders and non-LB-related diseases (ie, AD and MSA)



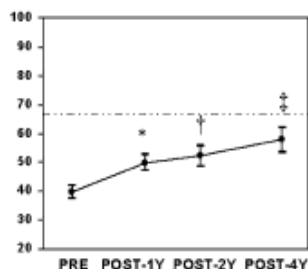
- 124 clinical samples drawn from 47 published studies.
- Data from 2965 subjects

- 123I-mIBG cardiac scintigraphy can accurately distinguish between **2 movement disorders, *Parkinson's disease and multiple system atrophy***, and between **2 common causes of dementia, *Alzheimer's disease and dementia with Lewy bodies***.
- H/M ratio threshold of 1.77 yielded 94% sensitivity and 91% specificity for the discrimination of these diagnostic clusters
- RBD's (rapid eye movement sleep behavior disorder) inclusion in the LB-related cluster suggests that it, too, may be an LB-related condition.

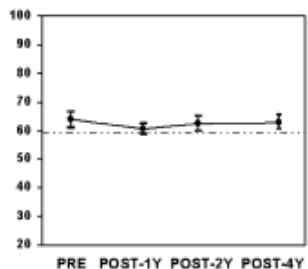
Dopamine Cell Implantation in Parkinson's Disease: Long-Term Clinical and ^{18}F -FDOPA PET Outcomes



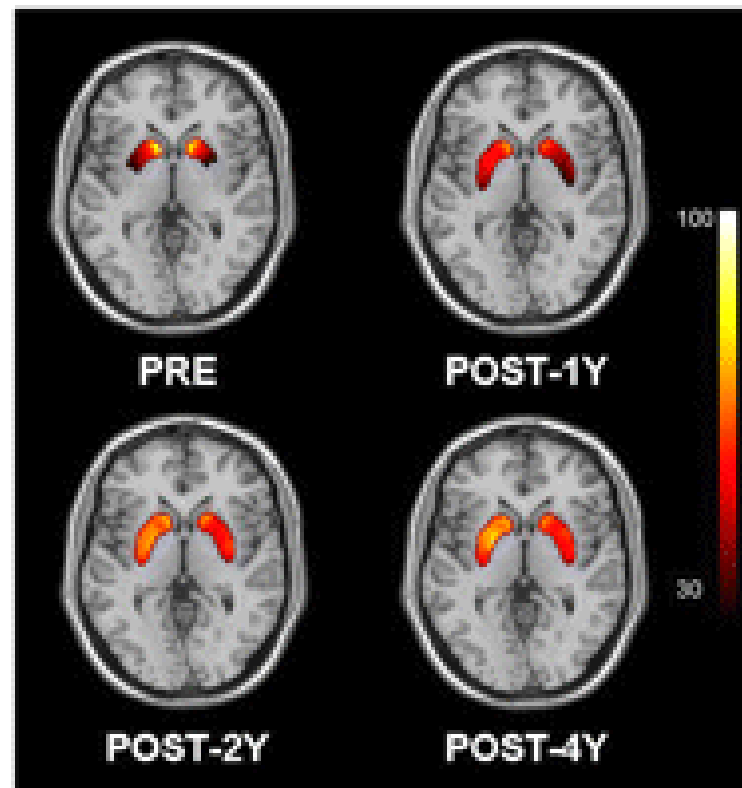
UPDRS motor ratings



Striatal ^{18}F -FDOPA uptake at baseline (pre) and at 1 (post 1 y), 2 (post 2 y), and 4 (post 4 y) years after bilateral implantation of fetal dopaminergic cells into putamen of PD patients.

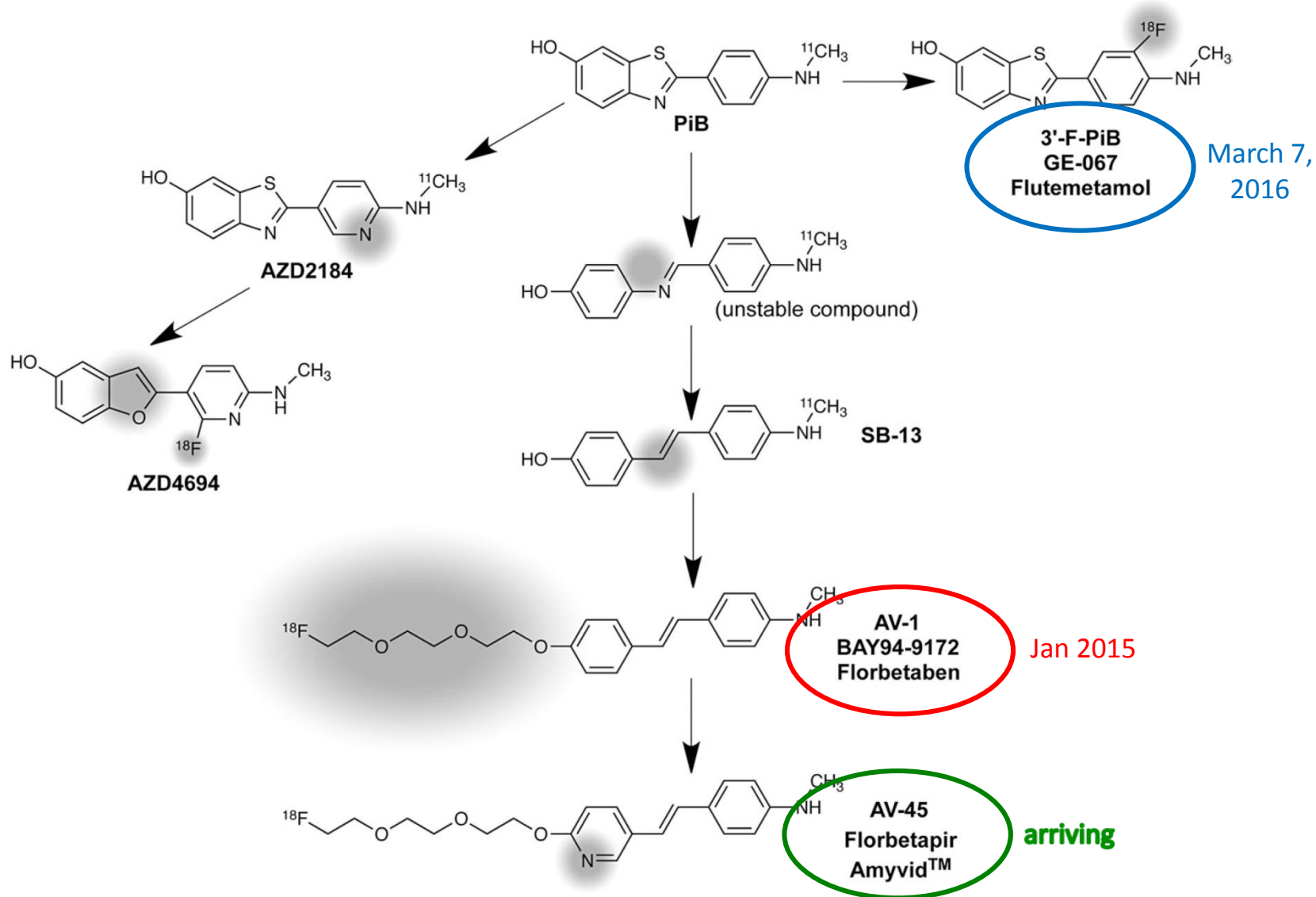


Nongrafted caudate after implantation



Significant treatment effect was noted over 2 y

PET amyloid tracers: fibrillar A β -amyloid deposition (Jan 2015)



Normal distribution (physiological uptake in white matter)
Regional retention reflects the regional density of amyloid plaques

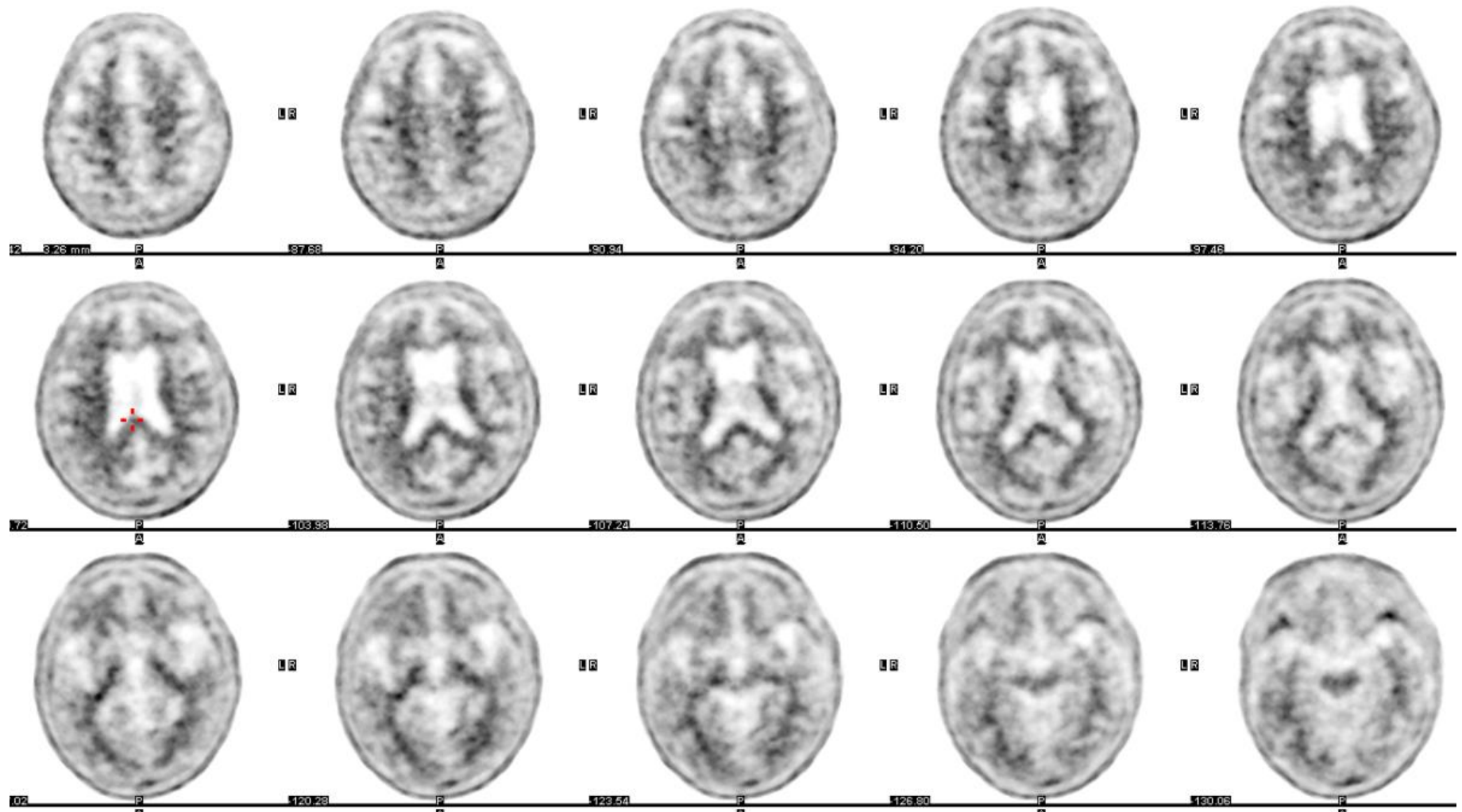


BAPL 1 (β Amyloid Plaque Load)

→ Qualitative regional grading score 1-4

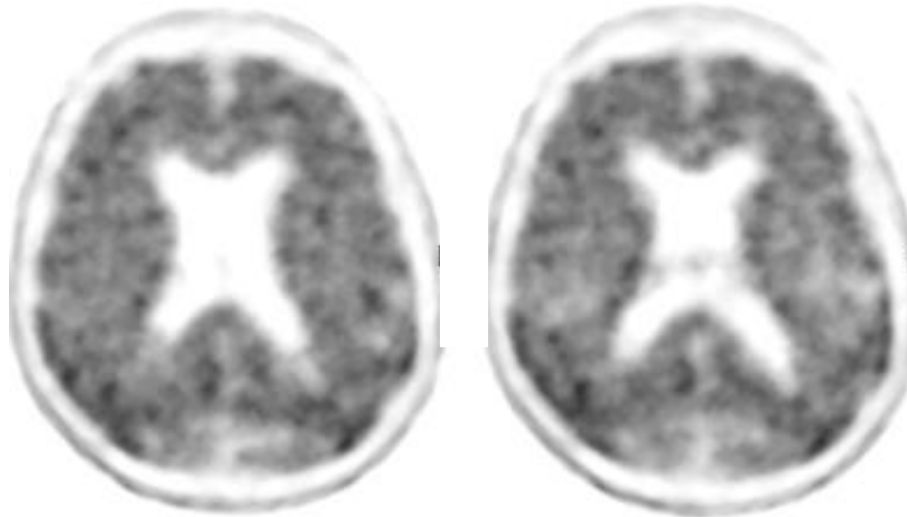
- Temporal
- Parietal
- Precuneus
- Frontal

→ Global assessment (BAPL) score 1-3

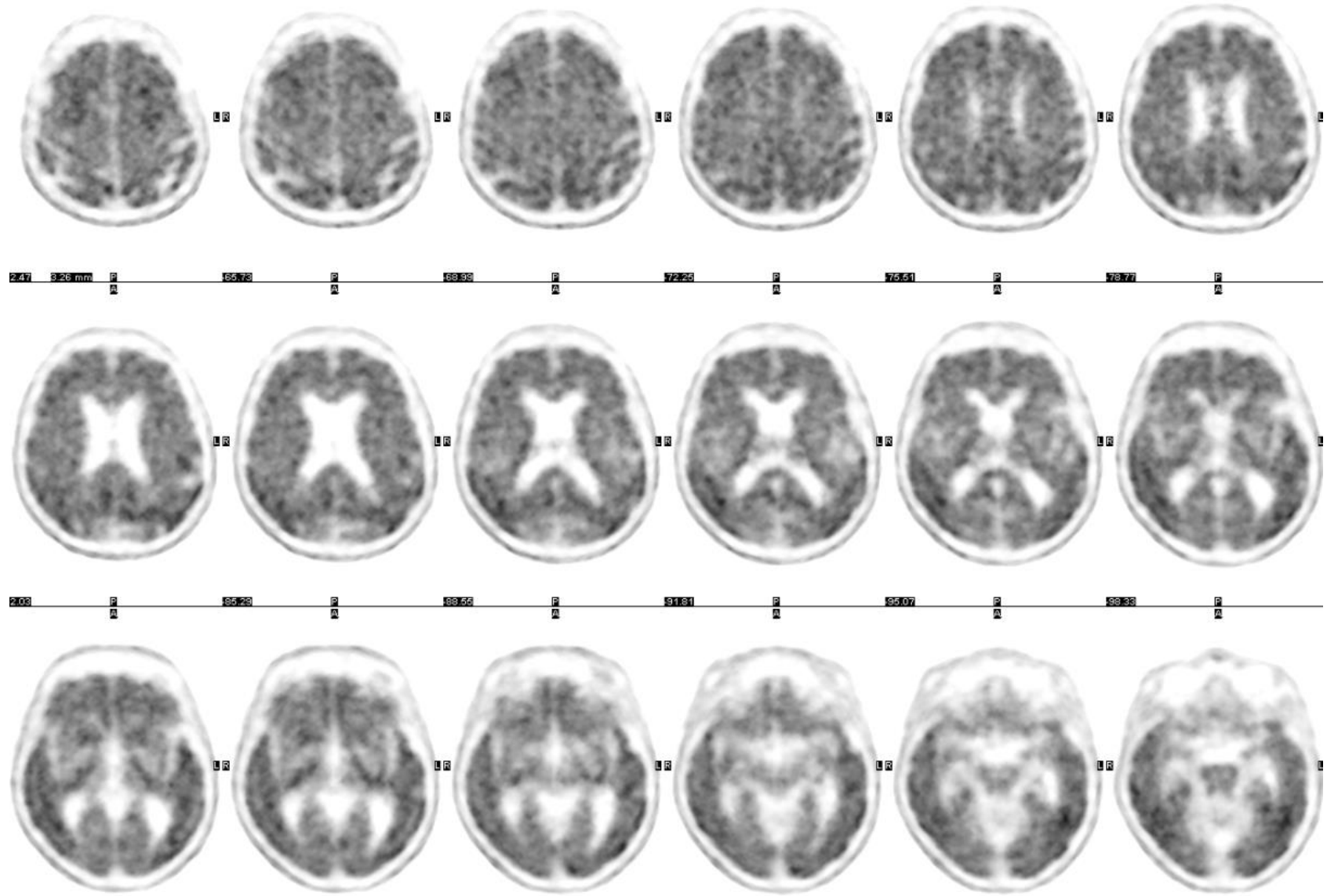


Normal distribution (physiological uptake in white matter)
Regional retention reflects the regional density of amyloid plaques

Cortical binding equal to or greater than white matter binding



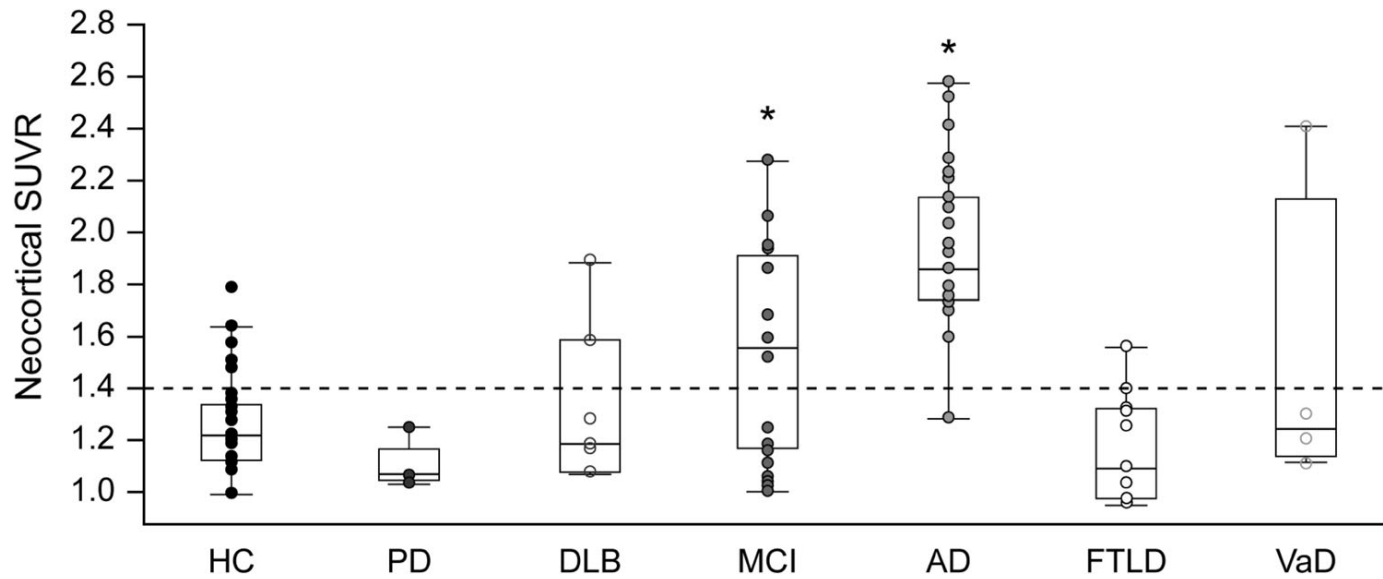
BAPL 3 (β Amyloid Plaque Load)



BAPL 3 (β Amyloid Plaque Load)

Critical binding equal to or greater than white matter binding

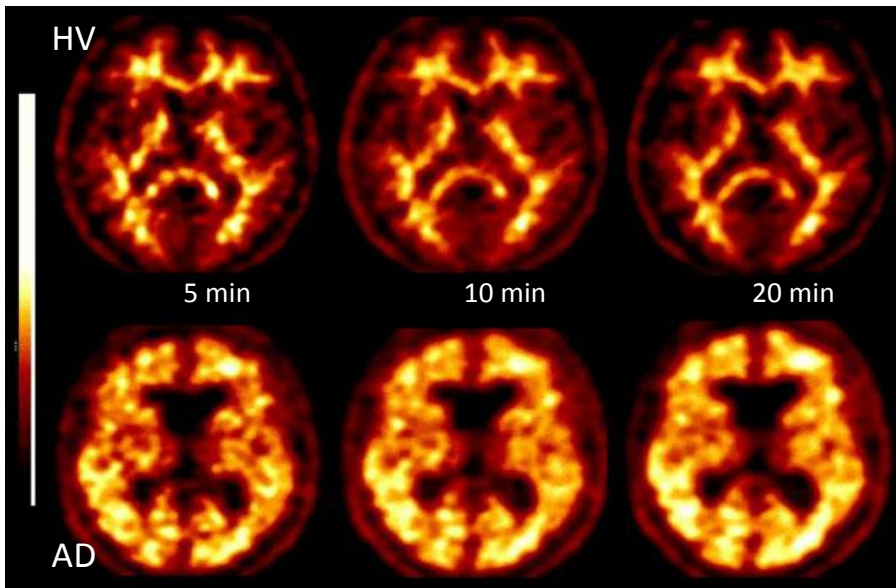
- Robust separation between AD patients and healthy age-matched control (HC) subjects both by visual image interpretation and simple quantitative measures
- Recently completed phase II clinical studies further confirmed these results.
- Matching the reported post-mortem distribution of A β plaques, FBB allows detection of AD pathology in the brain of subjects with a wide spectrum of neurodegenerative diseases



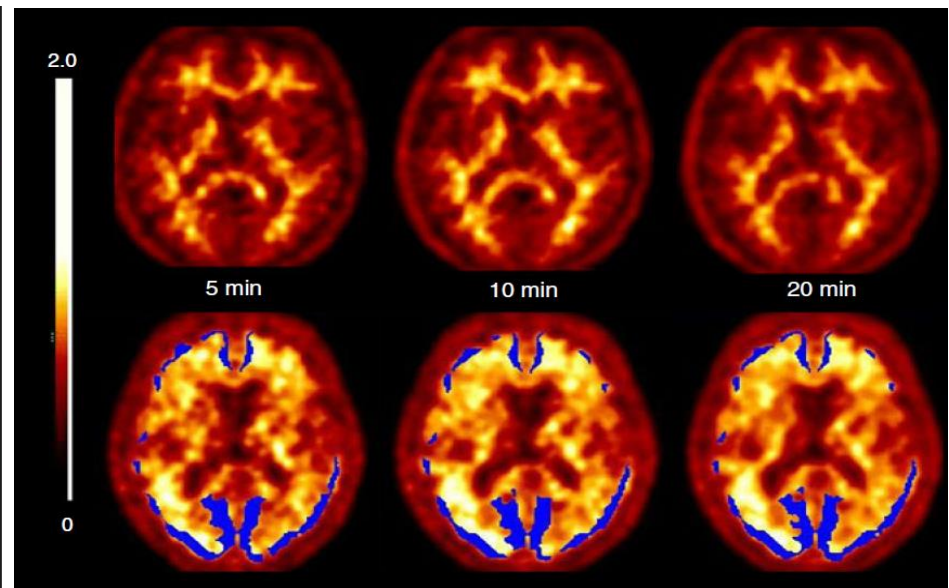
The influence of biological and technical factors on quantitative analysis of amyloid PET: Points to consider and recommendations for controlling variability in longitudinal data

Mark E. Schmidt^{a,*}, Ping Chiao^b, Gregory Klein^c, Dawn Matthews^d, Lennart Thurfjell^e, Patricia E. Cole^f, Richard Margolin^g, Susan Landau^h, Norman L. Foster^j, N. Scott Mason^j, Susan De Santi^k, Joyce Suhy^c, Robert A. Koeppe^l, William Jagust^h, for the Alzheimer's Disease Neuroimaging Initiative

- Measurement of subtle changes in amyloid burden requires quantitative analysis of image data.
- Reliable quantitative analysis of amyloid PET scans acquired at multiple sites and over time requires rigorous standardization of
 - acquisition protocols
 - subject management
 - tracer administration
 - image quality control
 - image processing and analysis methods



Scan duration 90 min after injection



Blue clusters represent brain regions with z-scores >2.5

PET amyloid tracers: visual assessment

Visual assessment of florbetaben PET images by three blinded readers in the whole-brain analysis group (n = 74)

	Estimate	95% Lower CI	95% Upper CI
Sensitivity (%)			
Majority read	97.9	93.8	100.0
Reader 1	97.9	93.8	100.0
Reader 2	100.0	92.5	100.0
Reader 3	97.9	93.8	100.0
Specificity (%)			
Majority read	88.9	77.0	100.0
Reader 1	88.9	77.0	100.0
Reader 2	85.2	71.8	98.6
Reader 3	85.2	71.8	98.6

Alzheimer's & Dementia 11 (2015)

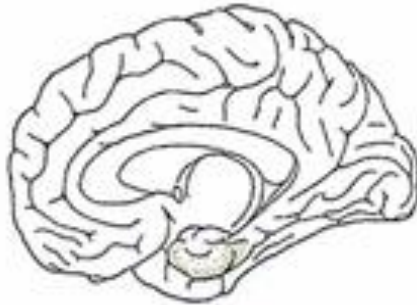
Inter-reader agreement in visual assessment of 18F-FBB images (n = 86)

	Amy+	Amy-	Severity Score 3	Severity Score 2
Major Reader	59	27	48	11
Reader 1	59	27	47	12
Reader 2	57	29	45	12

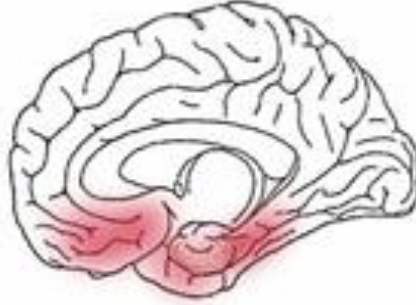
*AOU-PR
AIFA certified training*

Cerebral amyloid burden in Amnestic Mild Cognitive Impairment and Alzheimer's Disease

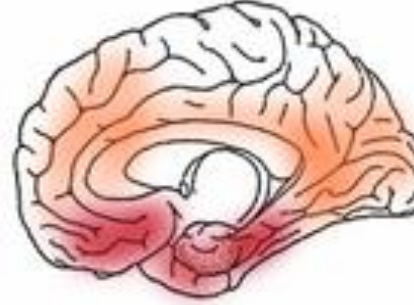
Stage 0



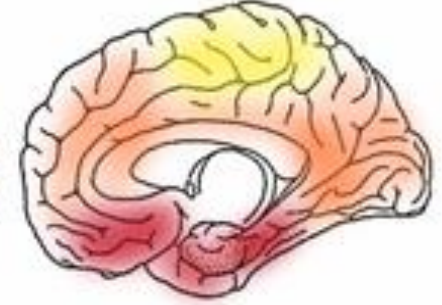
Stage A



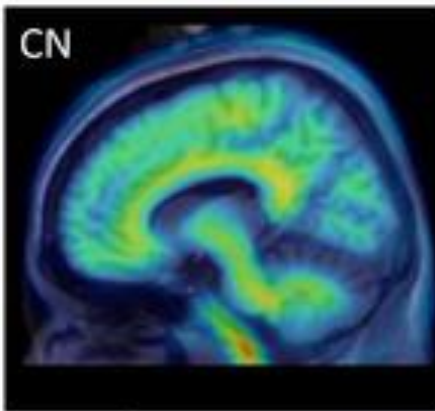
Stage B



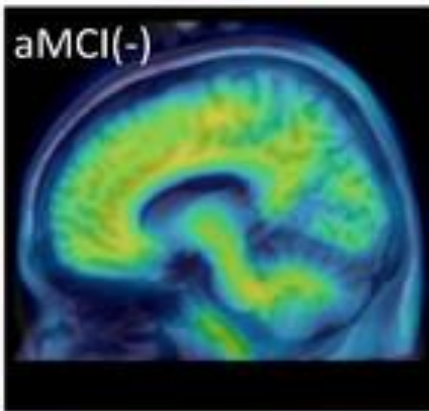
Stage C



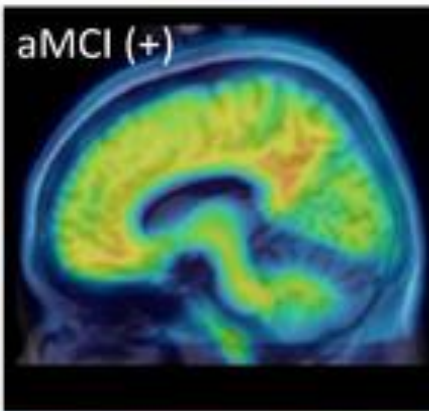
CN



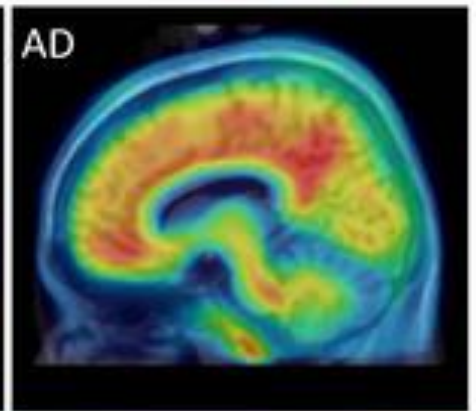
aMCI(-)



aMCI(+)



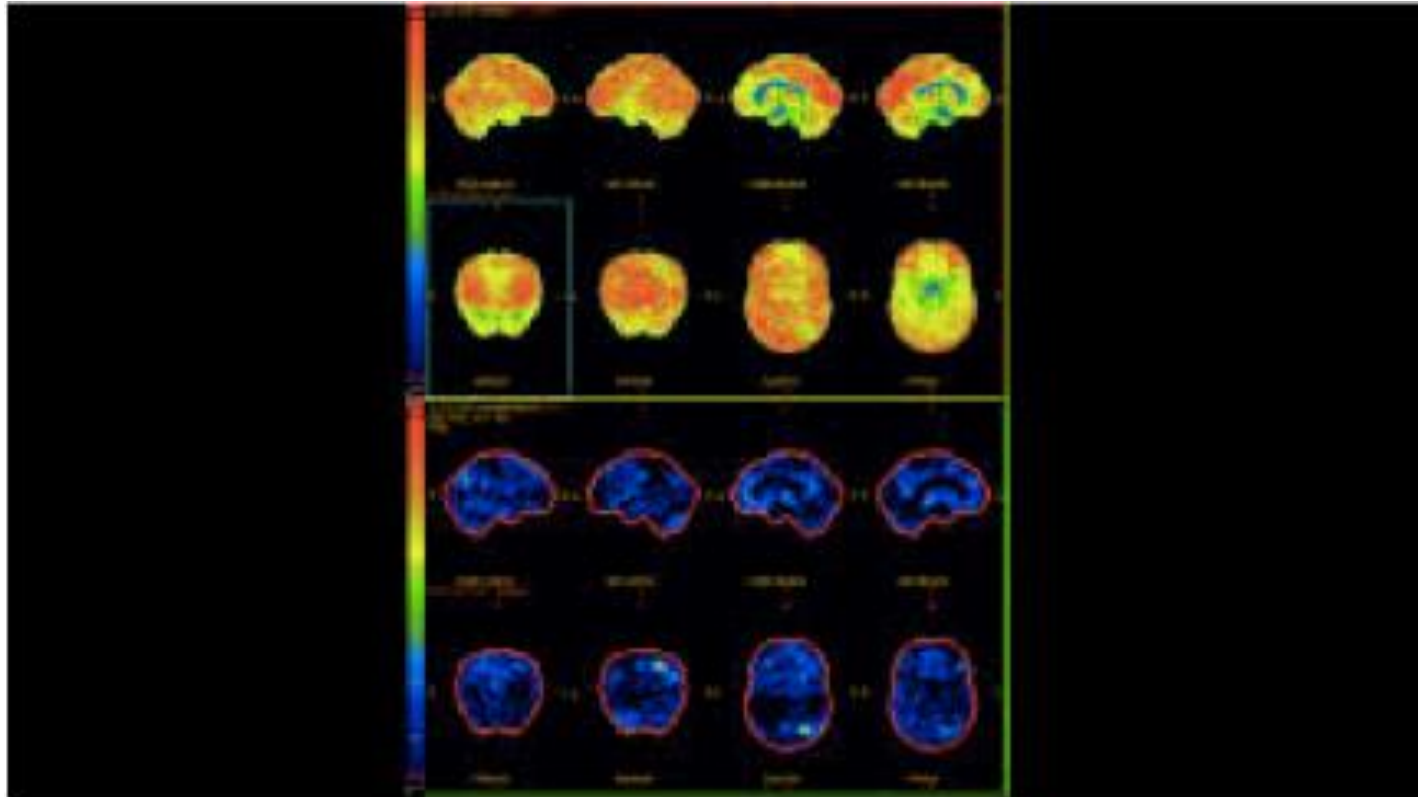
AD



QUANTITATIVE ANALYSIS

Method: Cortex ID Suite (GE Healthcare)

Normal database for ^{18}F -Flutemetamol



Quantitative maps with comparison to age-matched normals

QUANTITATIVE ANALYSIS (Normal)

Method: Cortex ID Suite (GE Healthcare)

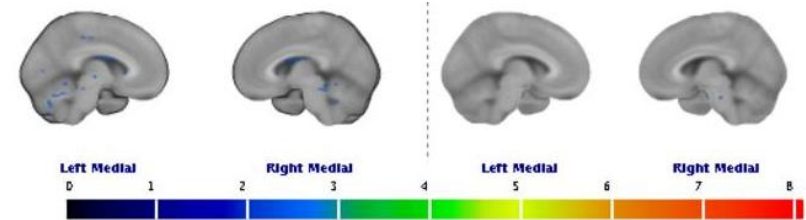
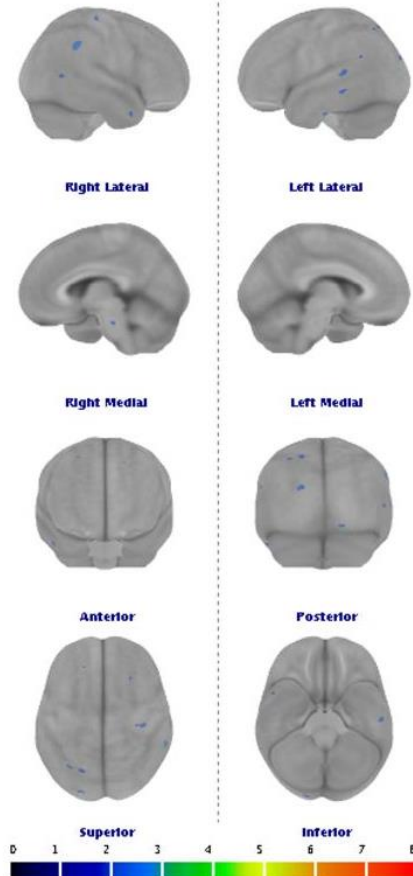
PET Flutemetamol Test Results

Ordering Provider : Not Available
 Reading Physician : VP 20 ml n
 Inj.Dose : 176.59 MBq/ml Flutemetamol

Age : 79
 Test Date : 09 May 2016
 Birth Date : 24 Aug 1936
 Exam : PET BRAIN VIZAMYL LATE
 Scanner : GE MEDICAL SYSTEMS Discovery IQ

Z-Score Images

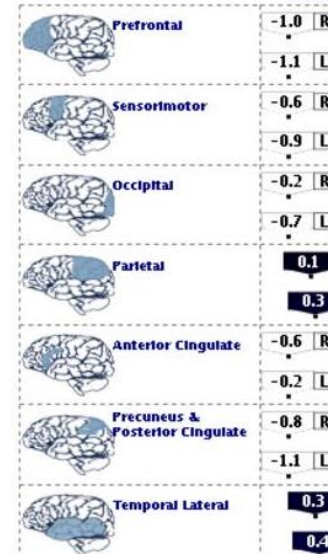
Region	Uptake Ratio	Z-Score
Composite	0.45	-0.53
Prefrontal R	0.43	-1.02
Prefrontal L	0.42	-1.10
Anterior Cingulate R	0.46	-0.55
Anterior Cingulate L	0.51	-0.22
Precuneus PostCing R	0.45	-0.53
Precuneus PostCing L	0.47	-1.11
Parietal R	0.51	0.12
Parietal L	0.50	0.25
Temporal Lateral R	0.54	0.28
Temporal Lateral L	0.54	0.40
Occipital R	0.53	-0.16
Occipital L	0.51	-0.74
Sensorimotor R	0.45	-0.57
Sensorimotor L	0.46	-0.59
Temporal Medial R	0.47	-1.39
Temporal Medial L	0.45	-1.03
Cerebellum Grey	0.36	-1.45
Cerebellum Whole	0.44	-1.17
Pons	1.00	0.00
Reference Region: Pons		



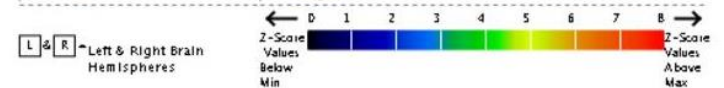
*Representative normal images have Z-scores for most brain areas less than 2 SD.
 Images shown have a 2 SD threshold applied

Z-Score Region Values

Standard Text



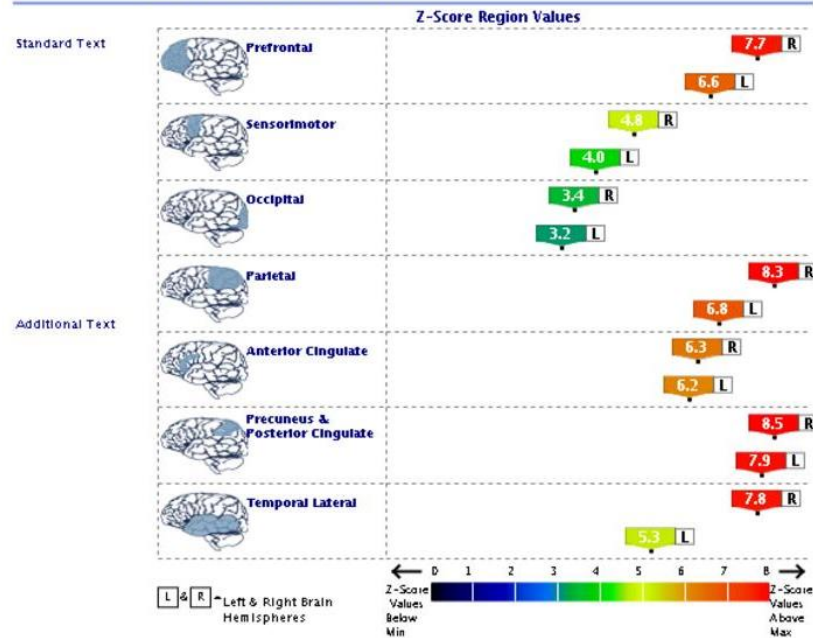
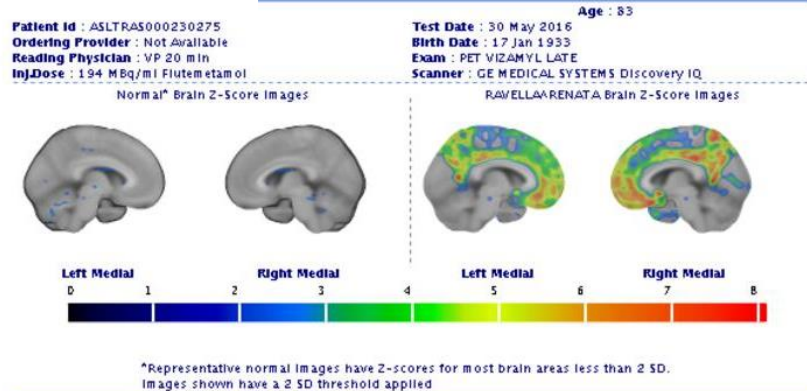
Additional Text



QUANTITATIVE ANALYSIS (AD)

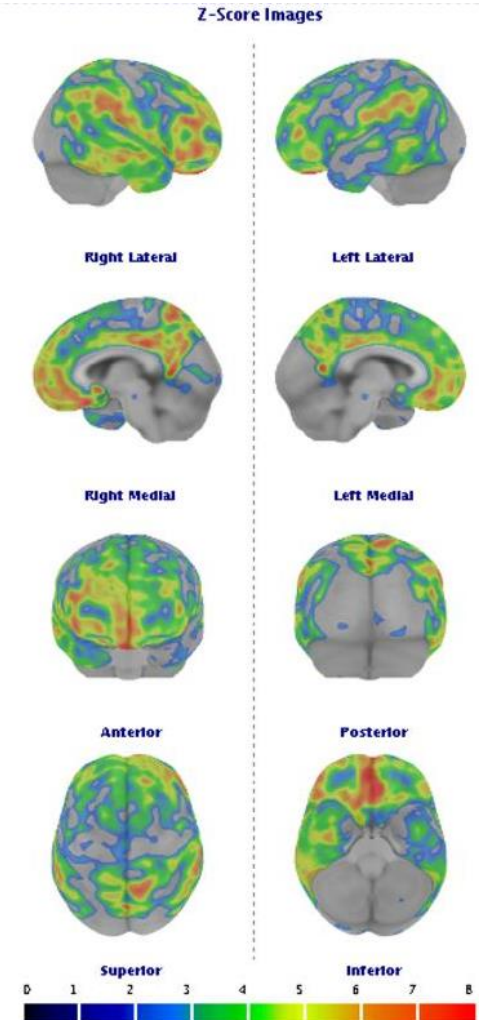
Method: Cortex ID Suite (GE Healthcare)

PET Flutemetamol Test Results

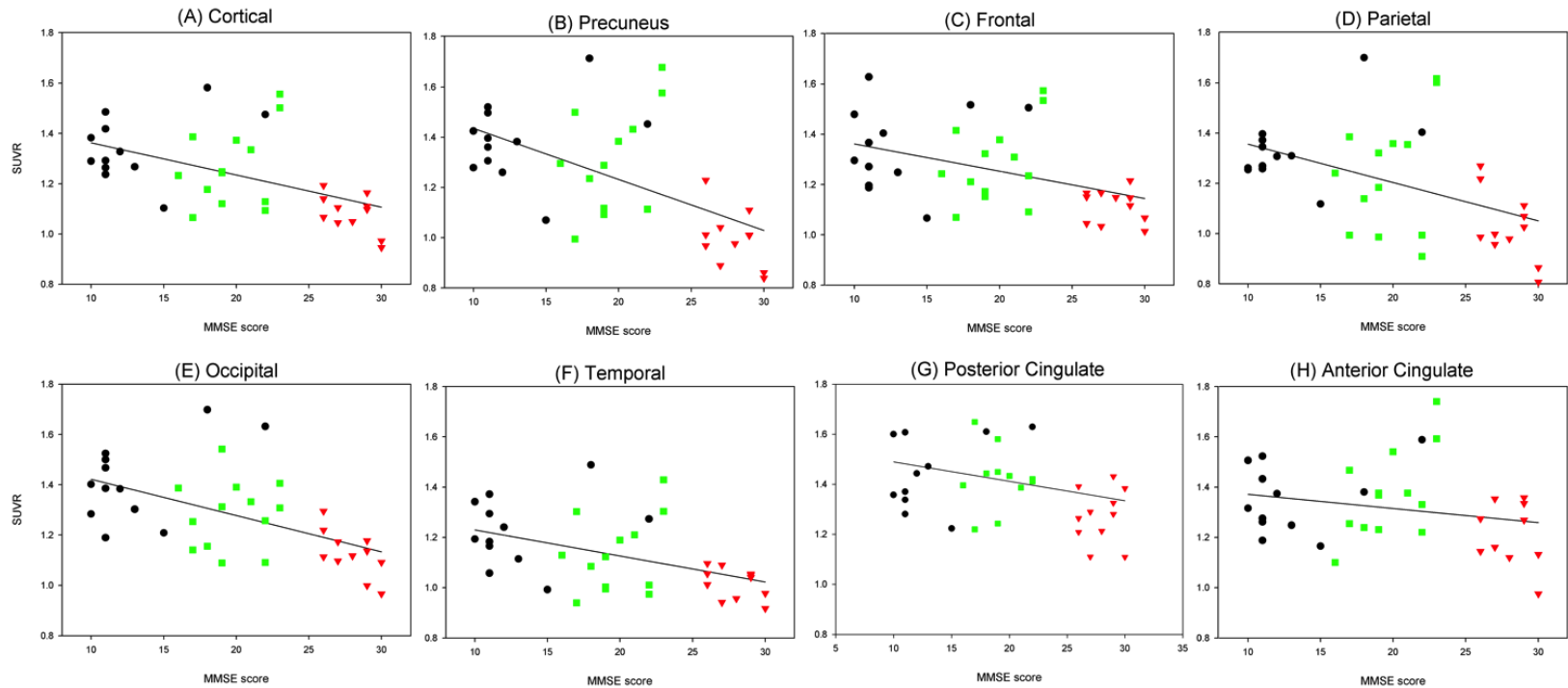


Region	Uptake Ratio	Z-Score
Composite	0.85	7.92
Prefrontal R	0.85	7.73
Prefrontal L	0.83	6.61
Anterior Cingulate R	0.85	6.34
Anterior Cingulate L	0.93	6.19
Precuneus PostCing R	0.94	8.54
Precuneus PostCing L	0.93	7.89
Parietal R	0.90	8.27
Parietal L	0.83	6.82
Temporal Lateral R	0.85	7.76
Temporal Lateral L	0.74	5.26
Occipital R	0.69	3.42
Occipital L	0.68	3.15
Sensorimotor R	0.76	4.84
Sensorimotor L	0.72	4.00
Temporal Mesial R	0.57	1.58
Temporal Mesial L	0.54	0.56
Cerebellum Grey	0.39	-0.32
Cerebellum Whole	0.50	0.71
Pons	1.00	0.00

Reference Region: Pons



Correlations between amyloid deposition and Cognitive Function



Negative correlation of MMSE scores with
SUVRs after adjustment for age and education

Multiple modality biomarker prediction of cognitive impairment in prospectively followed de novo Parkinson disease

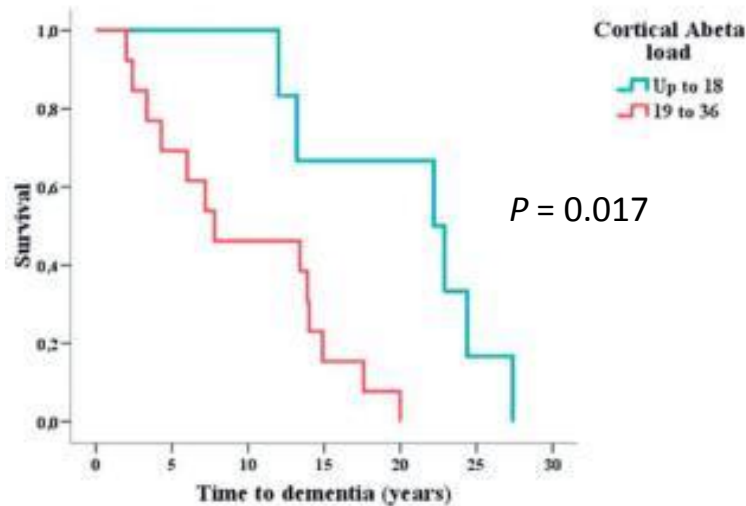
- **Cognitive impairment in PD increases in frequency 50–200%** in the first several years of disease, and is independently predicted by biomarker changes related to nigrostriatal or cortical dopaminergic deficits, global atrophy due to possible widespread effects of neurodegenerative disease, co-morbid Alzheimer's disease plaque pathology, and genetic factors.
- In Parkinson disease (PD) cognitive impairment can occur in a range of cognitive domains:
 - dementia (PDD) affects up to 80% of patients long-term
 - mild cognitive impairment (PD-MCI) occurs in 25–30% of non-demented patients and is a risk factor for dementia, and
 - cognitive deficits are present in some patients at the time of diagnosis.
- A range of demographic and clinical correlates or potential risk factors for cognitive decline have been identified, **increasing age and duration of PD, male sex, specific motor features** (postural instability gait disorder [PIGD] subtype), and a range of **non-motor symptoms** (e.g., visual hallucinations, apathy, depression, and rapid eye movement (REM) sleep behaviour disorder).
- Cortical Lewy body disease (LBD) pathology appears to be the major contributing pathology to cognitive decline in PD, but Alzheimer disease (AD)-related changes are also present in a significant percentage of patients.

Parkinson's Progression Markers Initiative (PPMI) <http://www.ppmi-info.org>

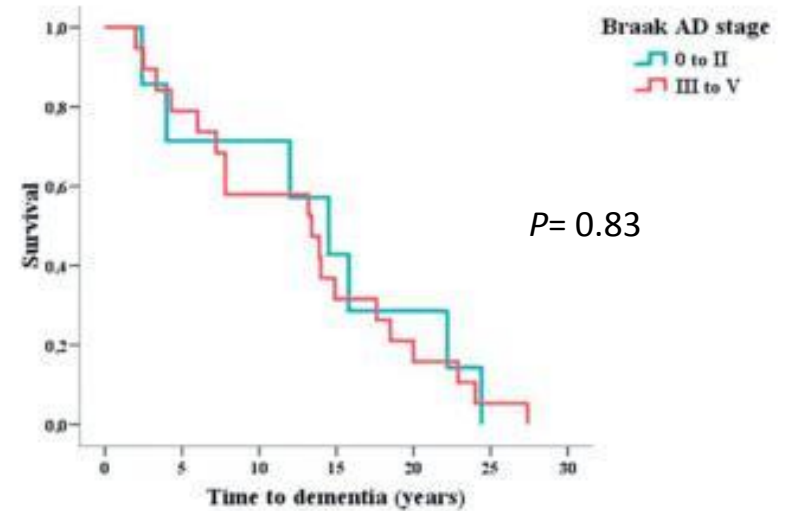
- ongoing, prospective, longitudinal, biomarker-rich observational study of disease progression in early PD
- up to 3 years, 423 newly diagnosed patients with idiopathic PD, untreated at baseline, from 33 international movement disorder centers

A β -amyloid load and survival analysis of time to dementia in patients with PD

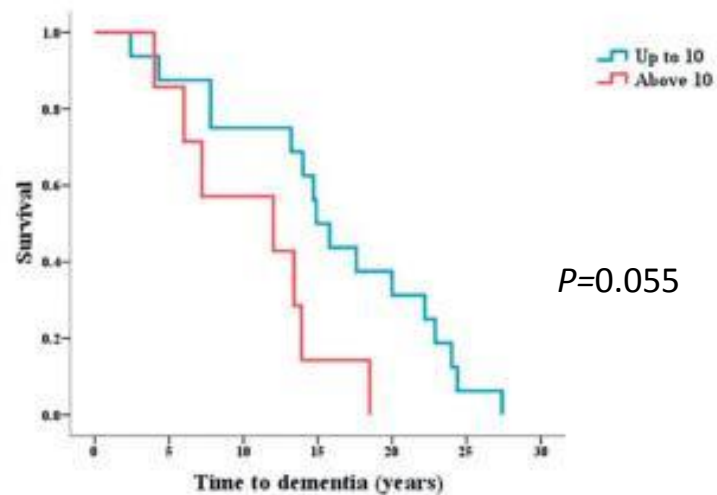
A Kaplan-Meier curve for time to dementia and cortical A- β load



B Kaplan-Meier curve for time to dementia and Braak AD (τ) stages



C Kaplan-Meier curve for time to dementia and cortical LB burden



Cerebral Amyloid Deposition Is Associated with Gait Parameters in the Mayo Clinic Study of Aging

Amy-PET SUVR, independent of general measures of AD-associated neurodegeneration, is associated with poorer performance on multiple gait parameters (speed, cadence, stride length, double support time, and intra-individual stance time variability) among cognitively normal women, aged 50 to 69 years.

Table 5. Cross-Sectional Association Between PiB-PET SUVR and Gait Parameters in Women After Adjusting for AD-Associated Neurodegeneration

ROIs	B (95% CI)				
	Gait Speed (N = 285)	Cadence (N = 285)	Stride Length (N = 285)	Double Support Time (N = 285)	Stance Time CoV (N = 284)
Prefrontal	-0.34 (-0.61, -0.07)*	-0.52 (-0.84, -0.21)**	-0.11 (-0.33, 0.12)	0.47 (0.14, 0.79)**	0.19 (0.05, 0.34)**
Orbitofrontal	-0.64 (-1.17, -0.11)*	-0.96 (-1.57, -0.35)**	-0.22 (-0.65, 0.21)	0.89 (0.27, 1.5)**	0.40 (0.12, 0.69)**
Parietal	-0.33 (-0.61, -0.04)*	-0.50 (-0.83, -0.17)**	-0.11 (-0.34, 0.13)	0.47 (0.14, 0.81)**	0.21 (0.06, 0.36)**
Temporal	-1.06 (-1.83, -0.28)**	-1.45 (-2.34, -0.55)**	-0.45 (-1.08, 0.17)	1.33 (0.42, 2.23)**	0.59 (0.17, 1.01)**
Anterior cingulate	-0.77 (-1.35, -0.19)**	-1.16 (-1.82, -0.49)**	-0.28 (-0.75, 0.19)	1.08 (0.41, 1.75)**	0.43 (0.12, 0.75)**
Posterior cingulate/ precuneus	-0.65 (-1.19, -0.12)*	-0.96 (-1.57, -0.35)**	-0.25 (-0.68, 0.18)	0.95 (0.33, 1.57)**	0.42 (0.14, 0.71)**
Motor ROI	-0.13 (-0.25, -0.02)*	-0.20 (-0.34, -0.07)**	-0.05 (-0.14, 0.05)	0.18 (0.05, 0.32)**	0.07 (0.008, 0.13)*

slower gait speed
(m/sec)

lower cadence
(steps/min)

longer double
support time
(sec)

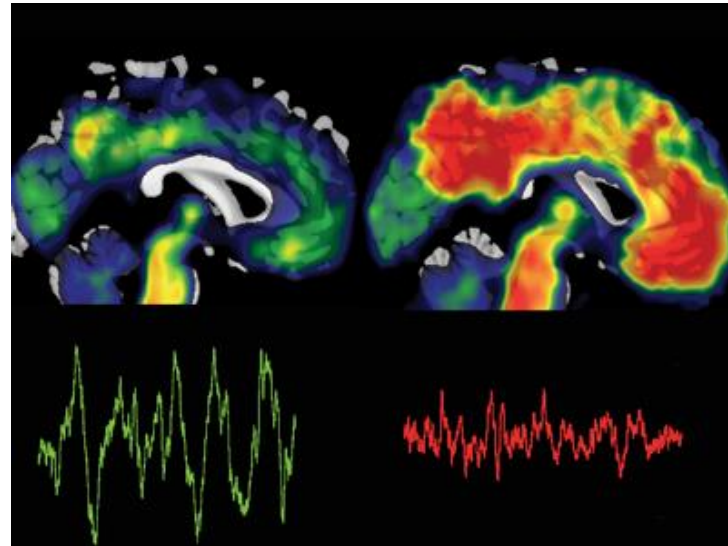
greater stance time
variability

Parkinson's Progression Markers Initiative (PPMI) <http://www.ppmi-info.org>

- ongoing, prospective, longitudinal, biomarker-rich observational study of disease progression in early PD
- up to 3 years, 423 newly diagnosed patients with idiopathic PD, untreated at baseline, from 33 international movement disorder centers

β -amyloid pathology relationship with both non-rapid eye movement (NREM) sleep disruption and memory impairment in older adults

Amy-PET



Normal
Sleep

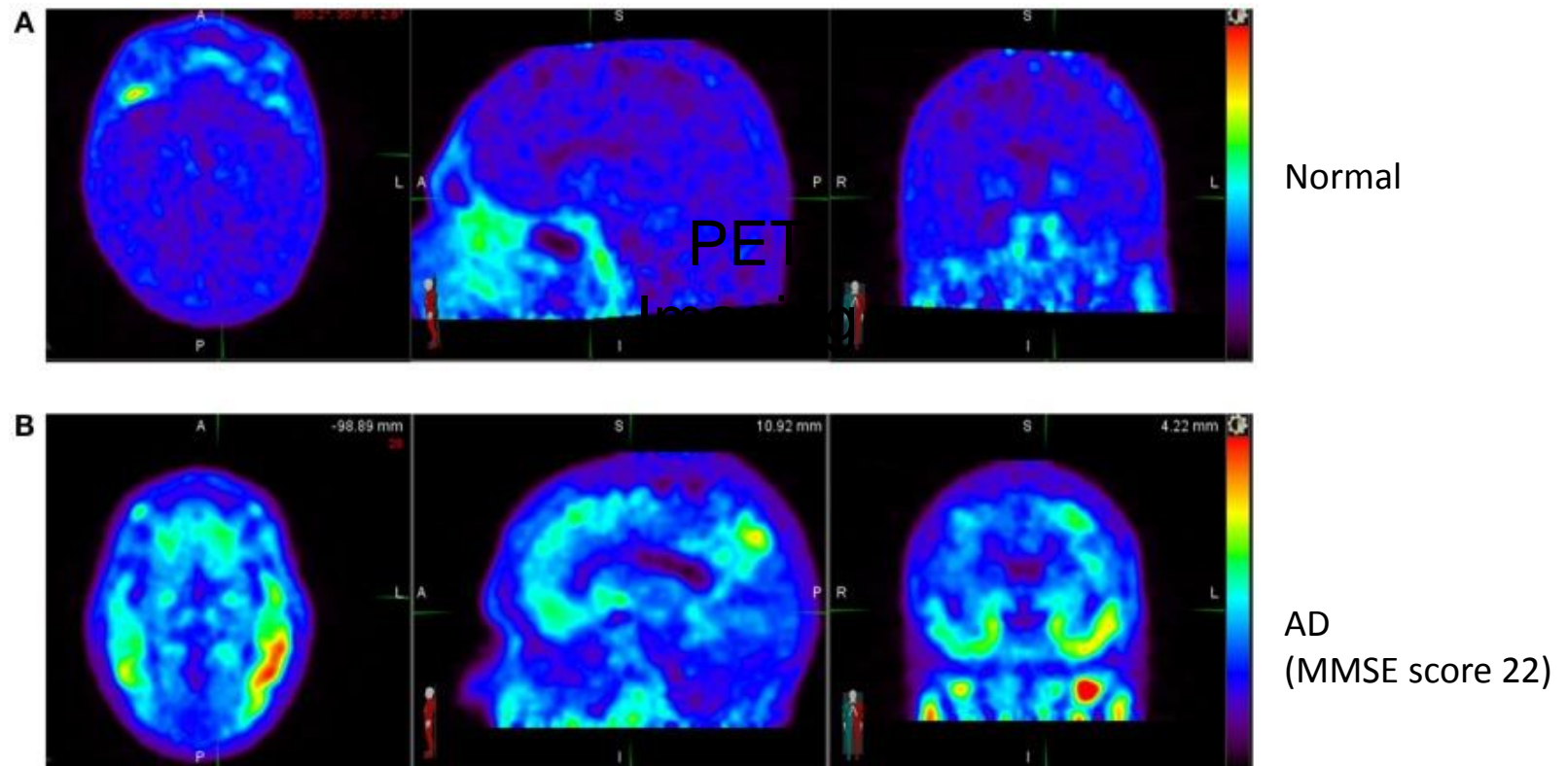
Amyloid deposition in poor sleep

- β -amyloid burden in medial prefrontal cortex (mPFC) correlates significantly with the severity of impairment in NREM slow waves generation.
- By linking β -amyloid pathology with impaired NREM SWA, these data implicate sleep disruption as a mechanistic pathway through which β -amyloid pathology may contribute to hippocampus-dependent cognitive decline in the elderly.

Arriving.....

PET Imaging of Tau Pathology in Alzheimer's Disease and Tauopathies

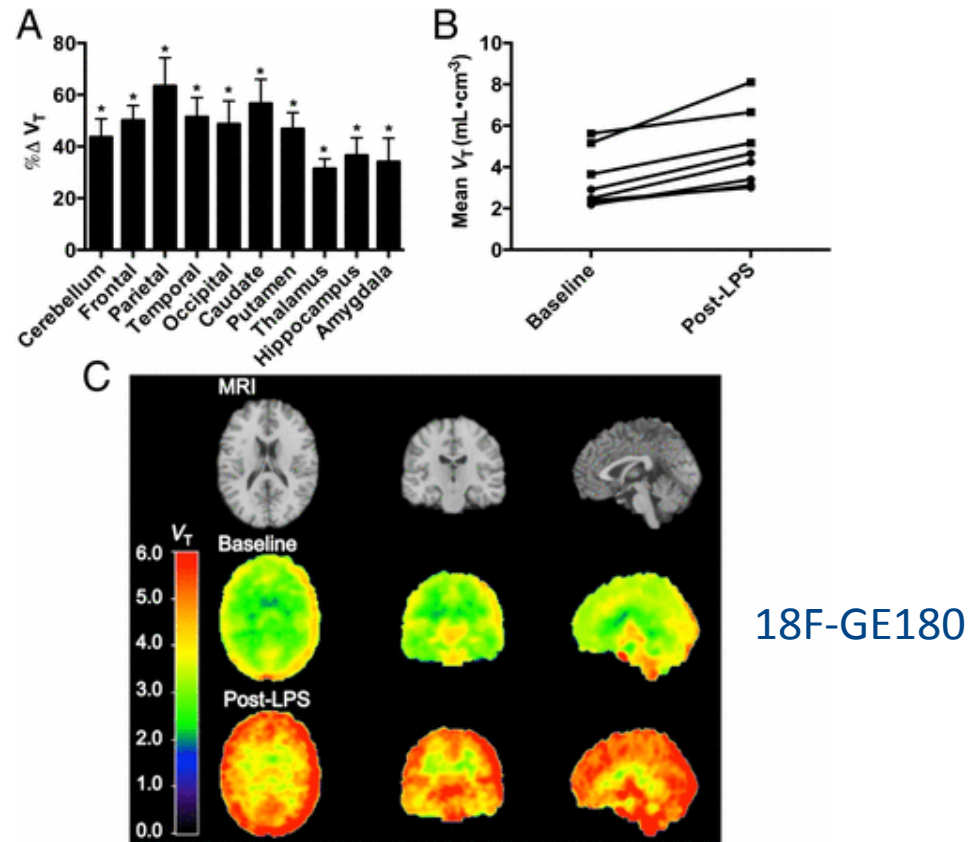
¹⁸F-AV-1451



Very low non-specific binding in white matter as well as cortical gray matter of healthy subjects

Arriving.....

Neuroinflammation imaging



Activation of microglia after administration of a potent immune activator (LPS)